

**NATURE OF SURFACE RHENIA SPECIES ON
SUPPORTED RHENIA CATALYSTS :
EFFECT OF OXIDE SUPPORT, LOADING AND ADDITIVES**

*A thesis submitted in Partial Fulfillment
of the Requirements for the
Degree of Master of Technology*

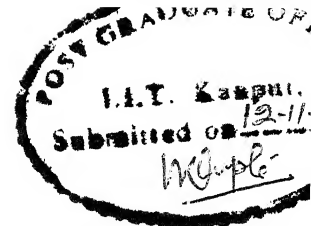
by

Brishti Mitra

to the

**Department of Chemical Engineering
Indian Institute of Technology, Kanpur**

November 1997



CERTIFICATE

It is certified that the work contained in the thesis entitled **Nature of Surface Rhedia Species on Supported Rhedia Catalysts : Effect of Oxide Support, Loading and Additives** by **Brishti Mitra** has been carried out under my supervision and that this work has not been submitted elsewhere for a degree.


Dr. Goutam Deo

Assistant Professor

Department of Chemical Engineering

Indian Institute of Technology, Kanpur.

November 12, 1997

5 MAR 1998 ICHE
CENTRAL LIBRARY
LAMPUR
Iss. No. A 125022

CHE-1997-M-MTT-NAT

Entered in system

On
6-4-98



A125022

Acknowledgements

I am extremely grateful to my advisor, Dr. Goutam Deo for his guidance and patience throughout my M.Tech project. Without his help and encouragement this work would not have been possible. I am also thankful to the other faculty members of the Chemical Engineering Department, especially Prof. M. S. Rao, Prof. D. Kunzru and Prof. J. P. Gupta for their help. My sincere thanks to Dr. A. Pradhan, Department of Physics for her valuable suggestions and counseling. I would also like to thank Prof. I. E. Wachs, Lehigh University, Bethlehem, PA, USA, for agreeing to have some of the experiments done at his laboratory.

The MHRD scholarship is gratefully acknowledged for the assistantship provided during my M. Tech studentship.

My special thanks goes to Loyd Burcham, Chuan Bao Wang, Xingtao Gao, Chaitali Roy and Nirmalya Ghosh for their help in carrying out some of the experiments.

I am also thankful to all my friends at IITK for making this stay a memorable one. Finally, I would like to thank my parents for their love, help and encouragement and my sister for just being there.

Abstract

The nature of the surface rhenia species on supported rhenia catalysts was determined as a function of oxide support, rhenia loading and additives. The catalysts were prepared using the incipient wetness impregnation method with dilute perrhenic acid as the precursor and characterized using Raman, FTIR and X-ray photoelectron spectroscopy, and TPR measurements. Raman and XPS studies reveal that the surface rhenia species are well dispersed on the Al_2O_3 and TiO_2 supports but the SiO_2 support was not successful in anchoring the rhenia species. Vibrational spectroscopic studies reveal that under ambient conditions the rhenia species is independent of oxide support (Al_2O_3 and TiO_2) and is similar to the rhenia species in aqueous solutions, namely the ReO_4^- species. Under dehydrated conditions the structure changes and an isolated, four-coordinated species with C_{3v} symmetry is proposed on both oxide supports independent of rhenia loading. This dehydrated surface species possesses three terminal $\text{Re}=\text{O}$ and a $\text{Re}-\text{O}$ -support bond. TPR measurements suggest that the reducibility of the surface rhenia species depends on the oxide support. The surface rhenia species on TiO_2 is more reducible than the rhenia species on Al_2O_3 . The difference in reducibility is related to the $\text{Re}-\text{O}$ -support bond strength. The additives, vanadium and sodium, can be categorized as interacting and non-interacting. The non-interacting additive (vanadium) directly coordinates to the oxide support without significantly affecting the surface rhenia species. The interacting additive (sodium), however, coordinates with the surface rhenia species changing its structure.

Contents

List of Figures	vii
------------------------	------------

List of Tables	x
-----------------------	----------

Chapter

1	Introduction	1
1.1	Applications and Characterization Techniques Used	1
1.2	Literature Review	3
1.3	Objectives and Thesis Outline	11
2	Experimental Procedure	13
2.1	Preparation of Catalyst Samples	13
2.2	X-Ray Photoelectron Spectroscopy (XPS) Studies	14
2.3	Raman Spectroscopy Studies	15
2.4	Fourier Transform Infra Red (FTIR) Spectroscopy Studies	16
2.5	Temperature Programmed Reduction (TPR) Studies	16
3	Results	19
3.1	XPS Studies	19
3.2	Raman Spectroscopy Studies	20
3.2.1	Ambient Conditions	20
3.2.2	Dehydrated Conditions	21
3.3	FTIR Spectroscopy Studies	22

3.3.1	Ambient Conditions	22
3.3.2	Dehydrated Conditions	22
3.3.3	Hydroxyl Region of $\text{Re}_2\text{O}_7/\text{Al}_2\text{O}_3$ and $\text{Re}_2\text{O}_7/\text{TiO}_2$ Catalysts	23
3.4	Temperature Programmed Reduction Studies	24
3.5	Effect of Additives	25
3.5.1	Rhenia-Vanadia-Titania and Rhenia-Vanadia-Alumina Catalysts	25
3.5.2	Sodium-Rhenia-Titania Catalysts	27
4	Discussion	53
4.1	XPS Studies	53
4.2	Oxide Supports and Rhenium Oxide Reference Compounds	54
4.3	Ambient Conditions	55
4.4	Dehydrated Conditions	57
4.5	Temperature Programmed Reduction Studies	59
4.6	Effect of Additives	61
5	Conclusions	66
	References	68

List of Figures

Fig. 2.1	Block Diagram Showing the Components of a Laser Raman Spectrometer	18
Fig. 3.1	XPS Surface Ratio Re/Al versus wt.% Re_2O_7	28
Fig. 3.2	XPS Surface Ratio Re/Ti versus wt.% Re_2O_7	29
Fig. 3.3	Raman Spectra of $\text{Re}_2\text{O}_7/\text{Al}_2\text{O}_3$ as a Function of Re_2O_7 Loading. Spectra Obtained Under Ambient Conditions.	30
Fig. 3.4	Raman Spectra of $\text{Re}_2\text{O}_7/\text{TiO}_2$ as a Function of Re_2O_7 Loading. Spectra Obtained Under Ambient Conditions.	31
Fig. 3.5	Raman Spectra of $\text{Re}_2\text{O}_7/\text{SiO}_2$ as a Function of Re_2O_7 Loading. Spectra Obtained Under Ambient Conditions.	32
Fig. 3.6	Raman Spectra of $\text{Re}_2\text{O}_7/\text{Al}_2\text{O}_3$ as a Function of Re_2O_7 Loading. Spectra Obtained Under Dehydrated Conditions.	33
Fig. 3.7	Raman Spectra of $\text{Re}_2\text{O}_7/\text{TiO}_2$ as a Function of Re_2O_7 Loading. Spectra Obtained Under Dehydrated Conditions.	34
Fig. 3.8	IR Spectra of $\text{Re}_2\text{O}_7/\text{Al}_2\text{O}_3$ as a Function of Re_2O_7 Loading in the Overtone Region. Spectra Obtained Under Dehydrated Conditions.	35
Fig. 3.9	IR Spectra of $\text{Re}_2\text{O}_7/\text{TiO}_2$ as a Function of Re_2O_7 Loading in the Overtone Region. Spectra Obtained Under Dehydrated Conditions.	36
Fig. 3.10	IR Spectra of $\text{Re}_2\text{O}_7/\text{Al}_2\text{O}_3$ in the Hydroxyl Region as a Function	37

of Re_2O_7 Loading.

Fig. 3.11	IR Spectra of $\text{Re}_2\text{O}_7/\text{TiO}_2$ in the Hydroxyl Region as a Function of Re_2O_7 Loading.	38
Fig. 3.12	TPR Profile for Different Weights of $20\%\text{Re}_2\text{O}_7/\text{Al}_2\text{O}_3$ Catalysts	39
Fig. 3.13	TPR Profile for $\text{Re}_2\text{O}_7/\text{Al}_2\text{O}_3$ Catalysts as a Function of Re_2O_7 Loading.	40
Fig. 3.14	TPR Profile for $\text{Re}_2\text{O}_7/\text{TiO}_2$ Catalysts as a Function of Re_2O_7 Loading.	41
Fig. 3.15	Raman Spectra of Vanadium Doped $\text{Re}_2\text{O}_7/\text{TiO}_2$ Catalysts Under Dehydrated Conditions. The Actual Legends of Each Spectrum Should Read (From Top to Bottom) : (a) $10\%\text{Re}_2\text{O}_7/1\%\text{V}_2\text{O}_5/\text{TiO}_2$ (b) $5\%\text{Re}_2\text{O}_7/1\%\text{V}_2\text{O}_5/\text{TiO}_2$ (c) $4\%\text{Re}_2\text{O}_7/\text{TiO}_2$ (d) $1\%\text{V}_2\text{O}_5/\text{TiO}_2$	42
Fig. 3.16	TPR Profile for Vanadium Doped $\text{Re}_2\text{O}_7/\text{TiO}_2$ Catalysts. The Actual Legends of Each Spectrum Should Read (From Top to Bottom): (a) $10\%\text{Re}_2\text{O}_7/\text{TiO}_2$ (b) $10\%\text{Re}_2\text{O}_7/1\%\text{V}_2\text{O}_5/\text{TiO}_2$ (c) $4\%\text{Re}_2\text{O}_7/\text{TiO}_2$ (d) $5\%\text{Re}_2\text{O}_7/1\%\text{V}_2\text{O}_5/\text{TiO}_2$ (e) $1\%\text{V}_2\text{O}_5/\text{TiO}_2$	43
Fig. 3.17	TPR Profile for Vanadium Doped $\text{Re}_2\text{O}_7/\text{Al}_2\text{O}_3$ Catalysts. The Actual Legends of Each Spectrum Should Read (From Top to Bottom): (a) $10\%\text{Re}_2\text{O}_7/\text{Al}_2\text{O}_3$ (b) $10\%\text{Re}_2\text{O}_7/1\%\text{V}_2\text{O}_5/\text{Al}_2\text{O}_3$ (c) $5\%\text{Re}_2\text{O}_7/\text{Al}_2\text{O}_3$ (d) $5\%\text{Re}_2\text{O}_7/1\%\text{V}_2\text{O}_5/\text{Al}_2\text{O}_3$ (e) $1\%\text{V}_2\text{O}_5/\text{Al}_2\text{O}_3$	44
Fig. 3.18	Raman Spectra of Sodium Doped $\text{Re}_2\text{O}_7/\text{TiO}_2$ Catalysts Under Ambient Conditions. The Actual Legends of Each Spectrum Should	45

Read (From Top to Bottom) : (a) 3%Na₂O/10%Re₂O₇/TiO₂

(b) 2%Na₂O/10%Re₂O₇/TiO₂ (c) 1%Na₂O/10%Re₂O₇/TiO₂

(d) 10%Re₂O₇/TiO₂

- Fig. 3.19 Raman Spectra of Sodium Doped Re₂O₇/TiO₂ Catalysts Under Dehydrated Conditions. The Actual Legends of Each Spectrum Should Read (From Top to Bottom):(a) 3%Na₂O/10%Re₂O₇/TiO₂ (b) 2%Na₂O/10%Re₂O₇/TiO₂ (c) 1%Na₂O/10%Re₂O₇/TiO₂ (d) 10%Re₂O₇/TiO₂ 46
- Fig. 3.20 Raman Spectra of 1%Na₂O/10%Re₂O₇/TiO₂ Catalysts Under Ambient and Dehydrated Conditions. 47
- Fig. 3.21 Raman Spectra of 2%Na₂O/10%Re₂O₇/TiO₂ Catalysts Under Ambient and Dehydrated Conditions. 48
- Fig. 3.22 Raman Spectra of 3%Na₂O/10%Re₂O₇/TiO₂ Catalysts Under Ambient and Dehydrated Conditions. 49
- Fig. 4.1 Stick Diagram of Rhenium Oxide Reference Compounds Having Different Structures. 63
- Fig. 4.2 Plot of Intensity of the Raman Band (Re=O Stretching Vibration) versus Attempted Rhenia Loading for Re₂O₇/TiO₂ and Re₂O₇/Al₂O₃ Catalysts. 64
- Fig. 4.3 Semilog Plot of TPR Peak Maxima versus Surface Concentration of Rhenium in the Re₂O₇/Al₂O₃ and Re₂O₇/TiO₂ catalysts. 65

List of Tables

Table 2.1	Oxide Support Specifications	17
Table 3.1	Attempted Concentration of Rhenium on Different Oxide Supports	50
Table 3.2	Atomic Concentration of Rhenium and Additives in Different Doped Supported Rhenia Catalysts	51
Table 3.3	Hydrogen Consumed by Different Supported Rhenia Catalysts During TPR Measurements	52

Chapter 1

Introduction

1.1 Applications and Characterization Techniques Used

Supported metal oxide systems constitute a very important class of heterogeneous catalysts. These catalysts are formed when a metal oxide is deposited on the surface of a second metal oxide substrate, that usually possesses a high surface area [1,2]. The deposited metal oxide component is considered to be the active phase of the catalyst and some such oxides are those of vanadium, rhenium, chromium, molybdenum, niobium, tungsten etc. The typical high surface area supports used are alumina, titania, silica, zirconia, niobia etc. These supported metal oxide catalysts find numerous applications in the petrochemical industry and for pollution control [3].

Supported rhenium oxide catalysts belong to this group of supported metal oxide catalysts. Here rhenium oxide (rhenia), the active component, forms a two dimensional overlayer on oxide supports such as alumina, silica, titania etc. The importance of these catalysts lie in their extensive use for the metathesis of olefins [4,5]. Olefin metathesis or olefin disproportionation reactions are industrially very important. These reactions provide an alternative way of producing useful compounds that cannot be synthesized from readily available starting materials by standard methods [6,7]. Tungsten oxide and molybdenum oxide catalysts are also used for metathesis of olefins but the superiority of

rhodium oxide is in its use under mild reaction conditions, viz., room temperature and atmospheric pressure. These conditions help reduce side reactions such as isomerization and polymerization, yielding exclusively the primary metathesis products [7]. Rhodium oxide catalysts are also used for several hydrotreating processes such as hydrodesulphurization [8,9] and hydrodenitrogenation [10]. Addition of rhodium improves the catalytic activity and stability of reforming catalysts containing platinum. Rhodium catalyzes cyclic ring opening and thus reduces coke formation. Rhodium oxide catalysts are also used as selective hydrogenation catalysts for several organic syntheses [11]. The catalytic activities of the supported rhodium catalysts for metathesis, is enhanced by the presence of other metal oxides like V_2O_5 , MoO_3 and WO_3 [12,13] and by the use of mixed oxide supports like $SiO_2 \cdot Al_2O_3$ and $Al_2O_3 \cdot B_2O_3$ [13,14,15]. Addition of MR_4 ($M = Sn$ or Pb ; $R = alkyl$) also helps in improving the activity of supported rhodium catalysts [13,14,15,16].

The industrial importance of the supported rhodium oxide catalysts has made it necessary to obtain fundamental information about the nature and functioning of the active sites, namely the surface rhodium species present. A knowledge of the surface composition and the local structure of the catalyst at the molecular level will help in better understanding the role played by the surface atoms in the catalytic reactions. The molecular level information can then be used for the design of better catalysts. The surface rhodium layer in the supported rhodium catalysts have been characterized by extended X-ray absorption fine structure (EXAFS) [17], X-ray absorption near edge spectroscopy (XANES) [17,18], Fourier transform infrared spectroscopy (FTIR) [19,20,21], uv-Visible

spectroscopy [19] and Raman spectroscopy [16,18,19,20,22,23]. Of these characterization techniques, Raman spectroscopy is most well-suited for the study of supported metal oxide catalysts and, consequently, supported rhenium oxide catalysts. The molecular nature of this characterization technique and its ability of discriminating between different metal oxide species that may simultaneously be present in the catalyst make Raman spectroscopy a very powerful characterization tool [24,25]. Infrared (IR) spectroscopic studies are also very useful but most of these studies are hampered by the absorption by the oxide support that obscures the metal-oxygen vibrations. IR spectroscopy can, however, detect those vibrations that are not Raman active due to the highly ionic nature of the bond in regions not obscured by absorption of the oxide support. Raman and IR spectroscopy also have the advantage of being carried out under *in situ* conditions. X-ray photoelectron spectroscopy helps in providing information about the dispersion of the oxide species on the support surface. The reduction properties of the supported rhenia catalysts can be determined by the Temperature Programmed Reduction (TPR) technique.

1.2 Literature Review

A brief review of the characterization studies involving supported rhenia catalysts with and without additives are given below in chronological order. The relevant points of the different studies are mentioned.

Olsthorn and Boelhouwer [26] sublimed Re_2O_7 onto the surface of alumina aerogel ($195 \text{ m}^2/\text{g}$). The loading was varied from ~20 to 26% Re_2O_7 by changing the temperature

of the alumina support. The characteristic vibrational bands of the surface hydroxyl groups of the alumina support was monitored by *in situ* IR spectroscopy and a monolayer coverage of $\sim 20\%$ Re_2O_7 was concluded. The monolayer coverage was inferred by observing when the hydroxyl bands characteristic of the alumina support were completely suppressed. The surface rhenia species at monolayer coverage was proposed to consist of small Re_2O_7 aggregates. Furthermore, surface rhenia species was found to be stable and could undergo oxidation and reduction cycles.

Yao and Shelef [27] examined low coverages (1.21-5.51% Re_2O_7) of $\text{Re}_2\text{O}_7/\text{Al}_2\text{O}_3$ catalysts by means of Electron Spin Resonance (ESR) Spectroscopy and TPR techniques. The catalysts were prepared by the wetness impregnation technique and the Re content determined by X-ray fluorescence. These authors reported the presence of two different phases of rhenia on the surface: a two dimensional dispersed phase and three dimensional crystallites. The dispersed phase was found to strongly interact with the alumina support to form a stable species. This phase can be reduced to Re^0 by hydrogen at $>500^\circ\text{C}$ and can be oxidized at 500°C to Re^{+4} but not to Re^{+7} . The crystallite phase can be oxidized to Re^{+7} and reduced to Re^0 by hydrogen at 350°C . The three dimensional phase can be dispersed into the two dimensional phase by oxidation followed by vacuum or inlet gas treatment at $>500^\circ\text{C}$.

A study on the structures of unpromoted and SnBu_4 (Bu=butyl) promoted $\text{Re}_2\text{O}_7/\text{Al}_2\text{O}_3$ catalysts (surface area $\sim 180 \text{ m}^2/\text{g}$) were carried out by Maksimov *et al.* [28] using differential thermal analysis (DTA, DTG), X-ray diffraction and Mossbauer Spectroscopy. The catalysts contained 10-20% Re_2O_7 and was prepared by the

impregnation method. The promoted catalysts contained 6% SnBu₄. From the DTG ,DTA data and X-ray diffraction results they concluded that the rhenium did not exist on the surface as Re₂O₇ particles but in the form of a tightly bound surface compound. From the Mossbauer spectral data of the Sn promoted catalysts they concluded that the adsorption sites on the Al₂O₃ support surface and the Re₂O₇/Al₂O₃ catalyst surface are the same (either surface hydroxyls or Lewis acid sites). However they did not say anything about the exact nature of the surface sites on these catalysts.

Shpiro *et al.* [29] carried out XPS studies on the supported rhenium oxide catalysts. They studied the influence of supports (SiO₂, Al₂O₃), starting materials (HReO₄, NH₄ReO₄, KReO₄, Ba(ReO₄)₂) and conditions of pretreatment (chemical environment, temperature, pressure) on the state of rhenium. Their study on 3.4 to 4.8% Re₂O₇ catalysts showed that the state of the initial and reduced rhenium on SiO₂ is markedly different from that on Al₂O₃ and is dependent on the rhenium oxide precursor. They inferred that the reducibility of rhenium on Al₂O₃ was much less than that on SiO₂ due to the stronger interaction of Re⁺⁴ with SiO₂.

Kerkhof *et al.* [22] were the first to carry out a laser Raman spectroscopic study on supported rhenium oxide on alumina. The catalysts used contained 6-18% Re₂O₇ on alumina. Characterization was carried out under ambient conditions where presence of tetrahedral ReO₄⁻ ions were suggested. It was proposed that the ReO₄⁻ species were the only species present on the alumina support and were dynamically distorted by either the support or the support hydroxyls. However, no correlation between the rhenia loadings and the peak intensities of the Raman spectra was noted.

Nakamura *et al.* [30] examined 2-20% $\text{Re}_2\text{O}_7/\text{Al}_2\text{O}_3$ catalysts by *in situ* IR spectroscopy. The spectra suggested that the Re-O stretching modes of the surface rhenia species were consistent with that of the perrhenate ion and crystalline Re_2O_7 . Only ReO_4^- species was proposed in catalysts containing less than 13% Re_2O_7 but at higher loading (~17%) excess Re_2O_7 was found. The IR spectra was, however, restricted to in the Re-O stretching region, $\sim 900\text{-}1100\text{ cm}^{-1}$, and used only $\text{ReO}_4^-(\text{aq.})$ and crystalline Re_2O_7 as reference compounds.

Wang and Hall [19] characterized rhenia alumina catalysts by means of laser Raman, infrared and uv-Visible reflectance spectroscopy under dehydrated conditions. They prepared catalysts with a rhenia content ranging from 0.3 to 2.9 Re/g by the equilibrium adsorption method. A monomeric distorted tetrahedral rhenium oxide structure, possibly with C_{3v} or C_{2v} symmetry, on the alumina surface was proposed. Spectral studies also revealed that the catalyst surfaces could be dehydroxylated at high temperatures and the catalysts returned to its initial state by readsorption of water. The temperature programmed reduction features revealed that most of the rhenia was reduced to the metallic state at 275°C but a very small amount of rhenia appeared to resist reduction up to 500°C .

Duquette *et al.* [31] conducted ESCA studies on SiO_2 (surface area $300\text{ m}^2/\text{g}$) and Al_2O_3 (surface area $190\text{ m}^2/\text{g}$) supported rhenia catalysts to determine the oxidation states of rhenium in the active catalyst. They found out that for both the supports partial reduction to Re^{+6} and Re^{+4} occurred from the Re^{+7} state of the freshly calcined catalysts on exposure to a reactant (octene-1). Coke formation was greater on the SiO_2 supported

catalysts than the Al_2O_3 supported ones.

Temperature programmed reduction studies were used to characterize the reducibility of rhenium oxide catalysts supported on SiO_2 , Al_2O_3 and carbon by Arnoldy *et al* [32]. They found that for dried catalysts the surface contained both monolayer type Re^{+7} species and NH_4ReO_4 crystallites. High temperature calcination resulted in the decomposition of NH_4ReO_4 , formation of Re^{+7} surface phase and Re_2O_7 clusters, and rhenium loss due to sublimation of Re_2O_7 . Difference in the reducibility of the various catalysts were caused by the strength of the Re^{+7} -support interaction which decreased in the order $\text{Al}_2\text{O}_3 > \text{SiO}_2 > \text{carbon}$. They also carried out studies to determine the activation parameters for reduction of $\text{Re}_2\text{O}_7/\text{Al}_2\text{O}_3$ catalysts [33].

Edreva-Kardjieva and Andreev [34] examined the surface rhenia species on alumina under oxidative precatalysis conditions by thermal analysis, XPS, IR and diffuse reflectance spectroscopy studies in order to propose a structure for the surface species. They suggested that a monolayer of surface aluminum mesoperrhenate, AlReO_5 is present on the surface under oxidative conditions. This structure is heat and moisture stable and does not get readily converted to metallic rhenium. On heating the catalysts in inert atmosphere or vacuum, Re^{+6} and Re^{+4} valence states were found to coexist with Re^{+7} . They carried out similar studies on the $\text{Re}_2\text{O}_7/\text{SiO}_2$ catalysts [35] and observed that under precatalysis conditions two different oxide structures were formed. A mixed surface rhenium oxide perrhenate phase containing Re^{+7} , Re^{+6} and Re^{+4} is formed on calcining in air, which is unstable to heat or moisture. On heating the samples in inert gas a mesoperrhenate structure is formed which is unstable and reducible.

X-ray adsorption near edge spectroscopy (XANES) and extended X-ray adsorption and fine structure (EXAFS) measurements have been carried out on the supported rhenium oxide on alumina by Ellison *et al.* [17]. Catalyst samples ranging from 2.5 to 15 wt% Re_2O_7 were prepared by the wet impregnation method using ammonium perrhenate as precursor. The spectroscopic measurements were done under ambient conditions on the Re L_3 edge for rhenium oxide on alumina. They found that the spectra for the high loading samples (10 and 15% Re_2O_7) calcined at 525°C resembled that of crystalline perrhenate, while for the low loading (2.5% Re_2O_7) samples, the spectra revealed a clustered structure similar to that of Re_2O_7 . For higher loadings the surface species had a three dimensional perrhenate structure and for lower loadings rhenia clusters resembling Re_2O_7 were formed.

Hardcastle *et al.* [18] examined the interaction of the surface rhenia with the alumina support with varying rhenium oxide loading, calcination temperature and environment using laser Raman spectroscopy and XANES. Catalysts containing 0.1-20% Re_2O_7 were prepared by the incipient wetness impregnation technique. Under ambient conditions, where adsorbed moisture is present, the surface rhenia species is present as $[\text{ReO}_4]_{\text{ads}}$ possessing C_{3v} symmetry. *In situ* studies revealed a shift in the Raman bands indicating an increase in the Re-O bond order. High calcination temperature resulted in a decrease in the surface coverage due to the removal of the surface rhenia species as gaseous dimeric Re_2O_7 .

Yide *et al.* [36] investigated the effect of pretreatment by helium and/or propene on the nature of the active sites in $\text{Re}_2\text{O}_7/\text{Al}_2\text{O}_3$ catalysts. They found that for He

pretreatment, catalysts with higher Re ion density show higher activity while for propene pretreatment, catalysts with low Re ion density are more active. The active sites created by the two pretreatments were proposed to be different. XPS studies further reveal that the surface species after reaction are composed of different valence states. However, no mention was made of the exact species responsible for the above reactions.

Vuurman *et al.* [20] carried out laser Raman, IR spectroscopy and TPR studies of Re_2O_7 supported on Al_2O_3 , SiO_2 , TiO_2 and ZrO_2 . Under ambient conditions, the surface rhenia species was hydrated, independent of coverage or support type and had a ReO_4^- ion structure. Under dehydrated conditions two surface rhenium oxide species were present for Al_2O_3 , TiO_2 and ZrO_2 supports while for SiO_2 support there was just one species. The concentration ratio of the two surface species was a function of coverage and they all possessed C_{3v} symmetry with three terminal Re-O bonds and one Re-O-support bond. TPR data further revealed that the Re-O-support bond strength decreases in the order $\text{Al}_2\text{O}_3 > \text{ZrO}_2 > \text{SiO}_2 > \text{TiO}_2$.

Turek *et al.* [37] studied the acidic properties of $\text{Re}_2\text{O}_7/\text{Al}_2\text{O}_3$ catalysts by IR spectroscopy. Analysis of the hydroxyl region of the IR spectra revealed that there is a sequential depletion of the alumina OH groups on increasing rhenia loading. The more basic hydroxyls are initially replaced followed by the neutral and acidic hydroxyls. Spectra of CO_2 chemisorbed on $\text{Re}_2\text{O}_7/\text{Al}_2\text{O}_3$ revealed that at low loadings, five different types of CO_2 species were present, while at higher coverages only two of the most abundant types were found. The spectra for the 15.6% Re_2O_7 sample which corresponds to almost monolayer coverage revealed no chemisorbed CO_2 species.

Spronk *et al.* [38] examined the effect of calcination temperature on the activity of a 6% $\text{Re}_2\text{O}_7/\text{Al}_2\text{O}_3$ catalyst for the metathesis of propene. They found that the activity can be increased at higher calcination temperatures. The optimal temperature lies between 1100 to 1200 K. Lower the wt% of rhenium higher was the optimal calcination temperature. This improvement in the activity was attributed to the nearly random distribution of the ReO_4 groups on all types of sites of the alumina surface on calcination.

Kim and Wachs [23] investigated the molecular structure of 1% Re_2O_7 on supports such as Al_2O_3 , TiO_2 , ZrO_2 , SiO_2 and MgO under ambient and dehydrated conditions by Raman spectroscopy. Under ambient conditions, the surface rhenia species was found to resemble the ReO_4^- ion in aqueous solution independent of the oxide support. Under *in situ* conditions, the surface rhenia structure changes to an isolated four coordinated rhenium oxide species with three terminal $\text{Re}=\text{O}$ bonds and one bridging $\text{Re}-\text{O}$ -support bond for all supports except MgO . For $\text{Re}_2\text{O}_7/\text{MgO}$ system, compounds are formed due to a strong acid-base interaction between the MgO species and support.

There appears to be a lack of characterization studies on promoted supported rhenia catalysts. However, a few representative studies exist on other promoted metal oxide catalysts. For example, Deo and Wachs [39] studied the effect of additives like niobia, silica, tungstena, potassium oxide and phosphorus oxide on the structure and reactivity of the surface vanadium oxide phase in $\text{V}_2\text{O}_5/\text{TiO}_2$ catalysts. Under dehydrated conditions, WO_3 , Nb_2O_5 and SiO_2 were found to act as noninteracting additives and coordinates directly to the oxide support without significantly interacting with the surface vanadium oxide phase. K_2O and P_2O_5 were found to be interacting additives which

directly coordinates with the surface vanadium oxide phase. Interacting additives were observed to either form compounds or poison the active site.

Studies involving catalytic reactions with promoted supported rhenia catalysts exist. Mol and co-workers [12,13,14,15] carried out extensive reaction studies to examine the catalytic activity of Re_2O_7 on Al_2O_3 , $\text{SiO}_2\cdot\text{Al}_2\text{O}_3$ and $\text{Al}_2\text{O}_3\cdot\text{B}_2\text{O}_5$ promoted with V_2O_5 , MoO_3 , WO_3 and MR_4 ($\text{M}=\text{Sn}$ or Pb ; $\text{R}=\text{alkyl}$). Addition of promoters and use of mixed supports was found to increase the activity of the catalysts.

Williams and Harrison [16] used Raman spectroscopy to study the structure of $\text{Re}_2\text{O}_7/\text{Al}_2\text{O}_3$ catalysts with and without tetramethyltin promoter. The precursor (NH_4ReO_4) was found to possess a tetrahedral oxidic rhenium species which gets distorted when the precursor is activated. Addition of tetramethyltin results in an additional band in the Raman spectra due to Re-Sn interaction.

1.3 Objectives and Thesis Outline

Acquiring fundamental information about supported metal oxide catalysts require that the surface metal oxide species be a well defined system. Based on the above mentioned research it is evident that the surface rhenia species is ideally suited for fundamental studies involving supported metal oxide catalysts. This is so since the surface rhenia species is isolated and complications occurring due to multiple, polymeric and ill-defined species do not arise. Consequently, the objectives of the present work is broadly classified as:

- (i) Synthesis of the surface rhenia species on different oxide supports (Al_2O_3 , TiO_2 ,

and SiO_2).

(ii) Characterization of the surface rhenia species as a function of rhenia loading and oxide support.

(iii) Synthesis of additives on supported rhenia catalysts. The additives considered in the present study are vanadium and sodium.

(iv) Characterization of the surface rhenia species and additives on the oxide support.

The objectives of the thesis is achieved in the following chapters. In Chapter 2, the experimental procedures used to synthesize and characterize the supported rhenia catalysts with and without additives are outlined. In Chapter 3, the results obtained from the synthesis and characterization of the different supported rhenia catalysts with and without additives are described. Chapter 4, discusses the results obtained. Furthermore, the information obtained from the different characterization techniques are brought together to provide a broader perspective of the surface rhenia species. Finally, in Chapter 5 the conclusions of the study are presented.

In each chapter the Figures and Tables are arranged at the end in numeric order. The references to past research work are accumulated and placed under a separate section called References. The references are numbered in the order they appear in the text.

Chapter 2

Experimental Procedure

2.1 Preparation of Catalyst Samples

The supported rhenium oxide catalysts were prepared by the incipient wetness impregnation technique. The precursor used was a 60-70% aqueous solution of perrhenic acid (HReO_4 , Aldrich, 99.98% purity) and the supports used were titania (Degussa, 55 m^2/g), silica (Degussa, 300 m^2/g) and γ -alumina (Harshaw, 180 m^2/g). The supports were pretreated with incipient volumes of double distilled water and then calcined at 450°C (TiO_2) or 500°C (Al_2O_3 , SiO_2) for 16 h. The support specifications are summarized in Table 2.1. The supports and the incipient volume of perrhenic acid solution were then intimately mixed. The samples were dried at room temperature for 16 h, followed by drying at 110°C for 7 h and at 200°C for 16 h. The $\text{Re}_2\text{O}_7/\text{TiO}_2$ samples were finally calcined at 450°C for 2 h and the $\text{Re}_2\text{O}_7/\text{Al}_2\text{O}_3$ and $\text{Re}_2\text{O}_7/\text{SiO}_2$ samples at 500°C for 2 h. The final catalysts were denoted as x% $\text{Re}_2\text{O}_7/\text{support}$ where x denotes the attempted Re_2O_7 loading in terms of weight of Re_2O_7 per gram catalyst.

The effect of additives were studied by adding sodium hydroxide (NaOH, 20% solution) to a 10% $\text{Re}_2\text{O}_7/\text{TiO}_2$ sample previously prepared as described above, and perrhenic acid solution to a previously prepared 1% $\text{V}_2\text{O}_5/\text{TiO}_2$ and 1% $\text{V}_2\text{O}_5/\text{Al}_2\text{O}_3$ samples [40]. Double distilled water was added to a NaOH and a HReO_4 solution

separately to form incipient wetness volumes of solutions. The incipient wetness volumes of the two solutions were added to the 10% $\text{Re}_2\text{O}_7/\text{TiO}_2$ and 1% $\text{V}_2\text{O}_5/\text{TiO}_2$ and 1% $\text{V}_2\text{O}_5/\text{Al}_2\text{O}_3$ catalysts. The drying and heating of the samples were performed under conditions similar to those for the $\text{Re}_2\text{O}_7/\text{TiO}_2$ catalysts. The catalysts were denoted as y% $\text{Na}_2\text{O}/10\% \text{Re}_2\text{O}_7/\text{TiO}_2$ where y% stands for the weight percent of Na_2O deposited based on the TiO_2 support and z% $\text{Re}_2\text{O}_7/1\% \text{V}_2\text{O}_5/\text{TiO}_2$ (or Al_2O_3) where z% Re_2O_7 denotes the weight percent rhenium oxide deposited based on the TiO_2 and Al_2O_3 support.

2.2 X-ray Photoelectron Spectroscopy (XPS) Studies

The near surface compositions of the rhenia titania and rhenia alumina catalysts were determined using X-ray photoelectron spectroscopy (XPS). An X-ray beam of predominantly MgK_α or AlK_α X-rays were used for this analysis [41]. The electron spectrometer was operated in the fixed analyzer transmission (FAT) mode. The specimens for this analysis were prepared by pressing the catalyst powder between a stainless steel holder and a polished single crystal silicon wafer. The samples were mounted and taken to a turbomolecular pumped airlock evacuated to a pressure of 1×10^{-7} torr. The holder was then installed in the vacuum chamber of a Model DS 800 XPS surface analysis system manufactured by Kratos Analytical Plc, Manchester, UK. The chamber was evacuated to a base pressure of $\sim 1 \times 10^{-9}$ torr. A hemispherical electron energy analyzer was used for electron detection.

2.3 Raman Spectroscopy Studies

Two Raman spectrometers were used in this study. The laser Raman spectra of the $\text{Re}_2\text{O}_7/\text{TiO}_2$, $\text{Re}_2\text{O}_7/\text{Al}_2\text{O}_3$ and $\text{Re}_2\text{O}_7/\text{SiO}_2$ catalysts under ambient and dehydrated conditions were obtained by means of an Argon ion laser (Spectra Physics, Model 165). The 514.5 nm line was used as the exciting source. The laser power delivered at the sample was 15-40 mW. The scattered radiation from the sample was collected and directed into a Triplemate Spectrometer (Spex, Model 1877) coupled to a optical multichannel analyzer (Princeton Applied Research, Model 1463) with an intensified photodiode array detector thermoelectrically cooled to -35°C . About 200 mg of the supported rhenia catalysts were pressed into self supporting wafers and placed in a rotating sample cell, to avoid local heating effects. The Raman cell used in this study was developed by Jehng et al. [42]. The cell was heated to a temperature of 400°C for 1 h and the Raman spectra was obtained. The entire procedure was performed in a stream of flowing oxygen (ultra high purity grade Linde gas) over the catalyst samples to ensure complete oxidation of the catalysts. A block diagram of the components of a laser Raman spectrometer is shown in Fig. 2.1.

A second Raman apparatus was used for obtaining the spectra of rhenia catalysts with sodium and vanadium additives. Here the Raman set up was the same as above except that the detector used was an end window type GaAs photomultiplier tube (RCA C31034) cooled to -30°C by the Peltier effect. The Raman cell used for this study was a modified version of the cell developed by Pal et al. [43]. Raman spectra under dehydrated conditions were recorded after heating the sample to $\sim 200^\circ\text{C}$. For each spectra

15 scans were averaged.

2.4 Fourier Transform Infra Red (FTIR) Studies

The Fourier Transform Infra Red (FTIR) spectra of the $\text{Re}_2\text{O}_7/\text{TiO}_2$ and $\text{Re}_2\text{O}_7/\text{Al}_2\text{O}_3$ under dehydrated conditions were recorded on a Biorad FTS-7 Spectrometer (resolution 2 cm^{-1} and accuracy in the peak position $\sim 2\text{ cm}^{-1}$). The samples were pressed into self supporting wafers ($30\text{-}40\text{ mg/cm}^2$) and mounted on an in situ IR cell developed by Burcham and Wachs [44]. Initially, pure oxygen was passed with the temperature being increased to 300°C and maintained for one hour. Two spectra were taken at intervals of one hour to see whether they were identical.

2.5 Temperature Programmed Reduction (TPR) Studies

Temperature Programmed Reduction (TPR) studies were carried out on the $\text{Re}_2\text{O}_7/\text{TiO}_2$, $\text{Re}_2\text{O}_7/\text{Al}_2\text{O}_3$, $\text{Re}_2\text{O}_7/\text{V}_2\text{O}_5/\text{TiO}_2$ and $\text{Re}_2\text{O}_7/\text{V}_2\text{O}_5/\text{Al}_2\text{O}_3$ samples. A mixture of 10% hydrogen/argon at 1 bar pressure was used in a TPR apparatus (Altamira Instruments, Model AMI-100). The weight of the sample varied from 5 to 100 mg. Various runs were carried out on a particular sample with decreasing sample weight in order to eliminate errors due to mass transfer limitations. The samples were precalcined *in situ* at 500°C in air for 15 minutes. The samples were then cooled to 50°C and dry argon was flushed to remove the air. A mixture of hydrogen and argon at a molar ratio 1:9 was then passed at a flow rate of $17\text{ }\mu\text{moles/sec}$. TPR measurements were carried out by increasing the temperature linearly at the rate of 10°C/min up to 600°C . The hydrogen

monitored using a thermal conductivity detector.

TABLE 2.1 OXIDE SUPPORT SPECIFICATIONS

Support	Supplier	Pretreatment Temperature (°C)	Surface Area (m²/g)
TiO ₂	Degussa	450	55
γ-Al ₂ O ₃	Harshaw	500	180
SiO ₂	Degussa	500	300

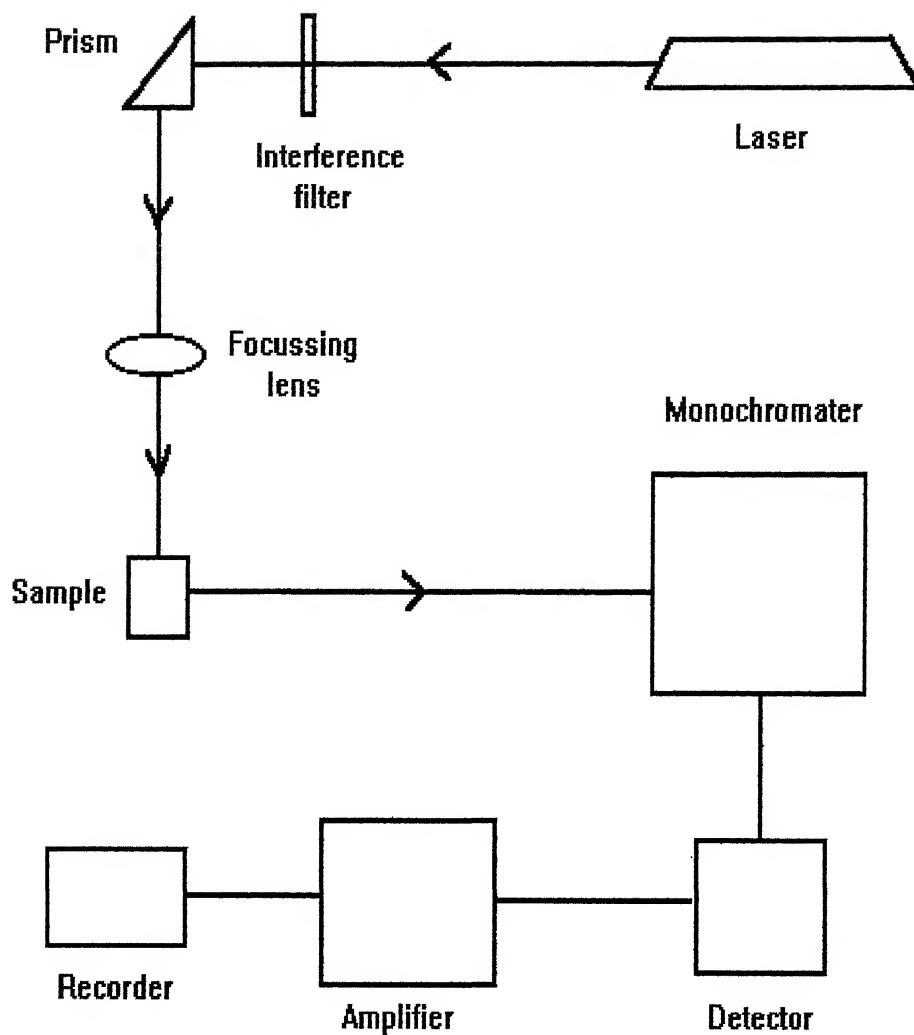


FIG. 2.1 BLOCK DIAGRAM SHOWING THE COMPONENTS OF A LASER RAMAN SPECTROMETER

Chapter 3

Results

Several loadings of rhenia on the Al_2O_3 , TiO_2 and SiO_2 supports were prepared. The attempted Re_2O_7 loadings on the different oxide supports are given in Table 3.1. Included in Table. 3.1 is the attempted rhenium concentration per unit surface area (atoms/nm²).

The vanadia and sodium doped catalysts were prepared to study the effect of additives. The loading of additives and rhenium on the different catalysts is shown in Fig. 3.2. Also included in Table 3.2 are the additive concentration and rhenium to additive atomic ratio (Re/V or Na).

3.1 XPS Studies

From XPS measurements the surface concentrations of atoms of the catalyst are determined. The XPS results of the $\text{Re}_2\text{O}_7/\text{Al}_2\text{O}_3$ and $\text{Re}_2\text{O}_7/\text{TiO}_2$ catalysts are shown in Figs. 3.1 and 3.2, respectively.

For the $\text{Re}_2\text{O}_7/\text{Al}_2\text{O}_3$ samples, the change in the surface Re/Al atomic concentration ratio with attempted loading of rhenium in the catalyst is shown in Fig. 3.1. The surface Re/Al ratio increases linearly with total rhenium oxide loading up to $\sim 10\%$ Re_2O_7 . After 10% and up to 20% Re_2O_7 , the slope reduces, noticeably and appears to be approaching

an asymptotic value.

In Fig. 3.2, the surface Re/Ti atomic concentration ratios are plotted against the attempted rhenium oxide loading for the $\text{Re}_2\text{O}_7/\text{TiO}_2$ catalysts. The surface Re/Ti ratio is seen to increase gradually up to $\sim 5\%$ Re_2O_7 , after which the slope reduces. Approaching 7% Re_2O_7 the curve has a decreasing trend.

XPS studies were not done on for the $\text{Re}_2\text{O}_7/\text{SiO}_2$ samples since all the Re_2O_7 on the SiO_2 support volatilizes as observed by Raman spectroscopy given below (Section 3.2.1).

3.2 Raman Spectroscopy Studies

Raman Spectroscopy provides information about the metal-oxygen vibrations in supported metal oxide catalysts. The region of interest is from 100 to 1200 cm^{-1} since metal-oxygen vibrations lie in this region.

3.2.1 Ambient Conditions

The Raman spectra of 1-20% $\text{Re}_2\text{O}_7/\text{Al}_2\text{O}_3$ are presented in Fig.3.3 from 200 to 1200 cm^{-1} . The major Raman bands are observed at 975, 930 and 339 cm^{-1} . The band positions and the relative intensities of the bands remain unaltered from 1 to 20% $\text{Re}_2\text{O}_7/\text{Al}_2\text{O}_3$, corresponding to low and high coverages of rhenia. The Raman spectra of 1-10% $\text{Re}_2\text{O}_7/\text{TiO}_2$ are shown in Fig.3.4 in the 700-1200 cm^{-1} region. Raman spectra below 700 cm^{-1} are not collected due to the very strong scattering from the TiO_2 support, which dominates this region. The spectra shows a strong band in the 977-991 cm^{-1} region

and a weak band at the 920 cm^{-1} region. The band at 796 cm^{-1} originates from the first overtone of the 395 cm^{-1} band of TiO_2 substrate [45]. All the Raman spectra are similar and independent of surface coverage except the 4% $\text{Re}_2\text{O}_7/\text{TiO}_2$ catalyst which shows two distinct peaks at 989 and 977 cm^{-1} .

The spectra for the 4% and 10% $\text{Re}_2\text{O}_7/\text{SiO}_2$ samples, shown in Fig.3.5, reveal bands at 977 , 806 , 604 , 490 and 438 cm^{-1} . These band positions are similar to the Raman bands of SiO_2 support. The silica support has very few reactive surface hydroxyls [46] and the surface rhenia species is known to volatilize easily [18]. It appears that a combination of these two factors result in no Raman bands of the surface rhenia species being present. This suggests that no rhenia species is present on the SiO_2 support. As a result no further characterization was done on the $\text{Re}_2\text{O}_7/\text{SiO}_2$ samples.

3.2.2 Dehydrated Conditions

The Raman spectra of the 1-20% $\text{Re}_2\text{O}_7/\text{Al}_2\text{O}_3$ catalysts under dehydrated conditions are presented in Fig.3.6 in the $600\text{-}1200\text{ cm}^{-1}$ region. A sharp band at $\sim 1000\text{ cm}^{-1}$ is observed for all the samples except the 1% $\text{Re}_2\text{O}_7/\text{Al}_2\text{O}_3$ catalyst. Additional Raman band at 973 cm^{-1} is observed, for the 15 and 20% $\text{Re}_2\text{O}_7/\text{Al}_2\text{O}_3$ catalysts. The Raman spectra of the 1% $\text{Re}_2\text{O}_7/\text{Al}_2\text{O}_3$ catalyst is weak and the band positions, if any, are not clearly discernable. The 1000 cm^{-1} and 973 cm^{-1} bands are assigned to the symmetric and asymmetric stretching modes of the terminal $\text{Re}=\text{O}$ bands, respectively [20].

The Raman spectra of the 1-10% $\text{Re}_2\text{O}_7/\text{TiO}_2$ samples under dehydrated conditions are shown in Fig.3.7 in the $700\text{-}1100\text{ cm}^{-1}$ region. The peak intensities in the spectra were

normalized to the TiO_2 peak at 643 cm^{-1} . The spectra reveal a strong band at 1003 cm^{-1} for catalysts of all rhenia loadings. This peak is assigned to the symmetric stretching mode of the surface rhenium oxide species. The asymmetric stretching mode expected at lower wavenumbers was not observed. The broad shoulder at the 795 cm^{-1} region is due to the TiO_2 support.

3.3 FTIR Spectroscopy Studies

FTIR spectroscopy like Raman spectroscopy is useful in observing metal-oxygen vibrations. However, limitations exist in using FTIR spectroscopy when oxide supports are present. FTIR spectroscopy is also useful in the hydroxyl region at $3100\text{-}3900\text{ cm}^{-1}$ where the behaviour of the support OH with metal oxide loadings can be observed.

3.3.1 Ambient Conditions

IR spectroscopy was not used as a characterization technique under ambient conditions since the bands of water and carbon dioxide interfere with the metal oxide bands under these conditions.

3.3.2 Dehydrated Conditions

The IR spectra of the 5-20% $\text{Re}_2\text{O}_7/\text{Al}_2\text{O}_3$ catalysts under dehydrated conditions is shown in Fig.3.8 in the first overtone region since the fundamental metal-oxygen vibrations are not clearly observed due to the strong absorption of the oxide support. For each of the spectra the background has been subtracted and the spectra smoothed. The

spectra shows the presence of two bands at ~ 1992 and 1954 cm^{-1} , which are assigned to the symmetric and asymmetric vibrations of the $\text{Re}=\text{O}$ vibrations. In the case of IR spectra, the asymmetric vibration is stronger than the symmetric one. Accordingly, the 1954 cm^{-1} peak (asymmetric stretching band) is more intense than the $\sim 1992\text{ cm}^{-1}$ band. The band positions are, however, not exactly double the values of the fundamental bands at 1000 and 973 cm^{-1} [20]. The difference may be due to the anharmonicity of the $\text{Re}=\text{O}$ vibrations.

In Fig. 3.9 the IR spectra for 1-7% $\text{Re}_2\text{O}_7/\text{TiO}_2$ catalysts is shown. There are two sharp bands at ~ 2004 and 1974 cm^{-1} similar to the spectra of $\text{Re}_2\text{O}_7/\text{Al}_2\text{O}_3$ catalysts. The ~ 2004 and 1974 cm^{-1} bands correspond to the symmetric and asymmetric vibrations, respectively. The 1974 cm^{-1} band corresponding to the asymmetric stretching mode is absent in the Raman spectra but can be clearly observed in the IR spectra. The intensity ratio of the ~ 2004 and 1974 cm^{-1} bands for the low loading $\text{Re}_2\text{O}_7/\text{TiO}_2$ samples are different from the $\text{Re}_2\text{O}_7/\text{Al}_2\text{O}_3$ samples.

3.3.3 Hydroxyl Region of $\text{Re}_2\text{O}_7/\text{Al}_2\text{O}_3$ and $\text{Re}_2\text{O}_7/\text{TiO}_2$ Catalysts

The hydroxyl region of the different supported rhenia catalysts are shown in Figs. 3.10 and 3.11. Fig. 3.10 shows the hydroxyl region of the $\text{Re}_2\text{O}_7/\text{Al}_2\text{O}_3$ catalysts with increasing loading going from top to bottom. Three of the hydroxyl bands due to the Al_2O_3 support at 3727 , 3675 and 3563 cm^{-1} [37] decrease with increasing Re_2O_7 loading and only a broad 3584 cm^{-1} band is observed for the 20% $\text{Re}_2\text{O}_7/\text{Al}_2\text{O}_3$ sample.

The hydroxyl region of the $\text{Re}_2\text{O}_7/\text{TiO}_2$ catalysts with increasing loading are

shown in Fig.3.11 in a similar fashion. The hydroxyl bands due to the TiO_2 support at 3720, 3662, 3630 and $\sim 3490\text{ cm}^{-1}$ decrease with increasing Re_2O_7 loading. The hydroxyl bands at higher wavenumbers (3720, 3662 and 3630 cm^{-1}) decrease more rapidly than the hydroxyl bands at lower wavenumbers. A single broad band at $\sim 3450\text{ cm}^{-1}$ is observed for the 7% $\text{Re}_2\text{O}_7/\text{TiO}_2$ catalysts.

3.4 Temperature Programmed Reduction Studies

Fig.3.12 shows the temperature programmed reduction profile of a 20% $\text{Re}_2\text{O}_7/\text{Al}_2\text{O}_3$ sample for different sample weights. The Thermal Conductivity Detector (TCD) signal per gram catalyst is plotted versus the sample temperature. Here the sample weights are varied in order to check for mass transfer limitations. The reduction peak maxima for the samples were observed at 338°C (0.005 gm), 345°C (0.011 gm) and 374°C (0.05 gm). Furthermore, two distinct peaks are also observed for the 0.05 gm sample suggesting a two stage reduction process. Clearly there is a shift in the peak maxima with respect to weight which is due to mass transfer limitations. Similar results were found for other weight percent catalysts. Thus, the data for the sample with the lowest weight was reported since this sample is least affected by mass transfer.

Fig.3.13 shows the TPR profiles for the $\text{Re}_2\text{O}_7/\text{Al}_2\text{O}_3$ catalysts as a function of Re_2O_7 loading (5-20%). A single sharp reduction peak was observed for all loadings of the sample. The TPR peak maxima is similar for all loadings ($337\text{--}361^\circ\text{C}$) within experimental error. The TPR patterns for the $\text{Re}_2\text{O}_7/\text{TiO}_2$ samples as a function of Re_2O_7 loading are presented in Fig.3.14. Sharp reduction peaks were observed for all samples.

The TPR peak maxima is observed to be similar for all loadings (191-224°C) within experimental error. No TPR band at ~90°C due to the presence of water was observed in any of the samples indicating that the supported rhenia samples were initially dehydrated [20].

A quantitative analysis of the TPR results for rhenia-titania and rhenia-alumina catalysts are shown in Table 3.3. The values of the atoms of hydrogen required per atom of rhenium reduced for different loadings show that the reduction of the Re is from the +7 state to a lower valence state but not to Re metal (zero valence state). However, these calculations are based on the attempted rhenium loading on the surface and not the actual amount of rhenium present and, hence, lead to valence states higher than the actual.

3.5 Effect of Additives

3.5.1 Rhenia-Vanadia-Titania and Rhenia-Vanadia-Alumina Catalysts

The Raman spectra of the 5 and 10% $\text{Re}_2\text{O}_7/1\% \text{V}_2\text{O}_5/\text{TiO}_2$ are shown in Fig.3.15 in the 700-1100 cm^{-1} region. The spectra of 1% $\text{V}_2\text{O}_5/\text{TiO}_2$ and 4% $\text{Re}_2\text{O}_7/\text{TiO}_2$ are included for reference. The spectrum of the unpromoted 4% $\text{Re}_2\text{O}_7/\text{TiO}_2$ catalysts exhibits a band at 1003 cm^{-1} due to the $\text{Re}=\text{O}$ vibration and that of 1% $\text{V}_2\text{O}_5/\text{TiO}_2$ catalyst, has a peak at 1028 cm^{-1} due to the $\text{V}=\text{O}$ vibration [39]. A sharp peak at ~1003 cm^{-1} is observed for both the rhenia-vanadia-titania samples which is similar to the 4% $\text{Re}_2\text{O}_7/\text{TiO}_2$ sample. Neither of the rhenia-vanadia-titania spectra show Raman features due to vanadium-oxygen vibrations. A closer look at the 5% $\text{Re}_2\text{O}_7/1\%\text{V}_2\text{O}_5/\text{TiO}_2$ spectra shows a slight shoulder at around ~1025 cm^{-1} which may be due to the addition of

vanadium oxide. There is a distinct shoulder around 796 cm^{-1} for all the cases which is due to the titanium-oxygen vibration as mentioned earlier.

The TPR patterns for the $\text{Re}_2\text{O}_7/\text{TiO}_2$ doped with V_2O_5 are presented in Fig.3.16. All the samples show a well defined peak indicating a one-step reduction. The TPR data for 1% $\text{V}_2\text{O}_5/\text{TiO}_2$, 4% $\text{Re}_2\text{O}_7/\text{TiO}_2$ and 10% $\text{Re}_2\text{O}_7/\text{TiO}_2$ have been included for reference. The TPR peak maxima for the 4% and 10% $\text{Re}_2\text{O}_7/\text{TiO}_2$ samples are at 216°C and 224°C , respectively. The reduction temperatures for the 5% $\text{Re}_2\text{O}_7/1\% \text{V}_2\text{O}_5/\text{TiO}_2$ and 10% $\text{Re}_2\text{O}_7/1\% \text{V}_2\text{O}_5/\text{TiO}_2$ samples are seen at 267°C and 258°C , respectively. The TPR peak for the 1% $\text{V}_2\text{O}_5/\text{TiO}_2$ is at a much higher value of 431°C . No reduction peaks in this region are observed for the vanadia doped samples. Due to the presence of vanadia, however, the reduction peaks seem to have shifted to a higher value implying that the reducibility of the rhenium oxide surface species is slightly affected.

Fig.3.17 shows the TPR profile for the vanadia doped $\text{Re}_2\text{O}_7/\text{Al}_2\text{O}_3$ catalysts. The patterns for the 1% $\text{V}_2\text{O}_5/\text{Al}_2\text{O}_3$, 5% $\text{Re}_2\text{O}_7/\text{Al}_2\text{O}_3$ and 10% $\text{Re}_2\text{O}_7/\text{Al}_2\text{O}_3$ are included for reference. While the other four samples show very intense single reduction peaks, the reduction peak at 530°C for the 1% $\text{V}_2\text{O}_5/\text{Al}_2\text{O}_3$ is hardly visible. Similar to the previous case of rhenia-vanadia-titania catalyst, the reduction temperatures get shifted to slightly higher values due to the influence of the vanadia species. No peaks at around 530°C are observed for either of the rhenia-vanadia-alumina samples.

The Raman spectra of vanadia doped $\text{Re}_2\text{O}_7/\text{Al}_2\text{O}_3$ catalyst could not be obtained due to fluorescence problems.

3.5.2 Sodium-Rhenia-Titania Catalysts

The Raman spectra of samples with increasing amounts of sodium added to 10% $\text{Re}_2\text{O}_7/\text{TiO}_2$ are shown in Fig.3.18 along with the 10% $\text{Re}_2\text{O}_7/\text{TiO}_2$ spectra for reference. These spectra were taken under ambient conditions. The 10% $\text{Re}_2\text{O}_7/\text{TiO}_2$ shows a distinct peak at $\sim 983\text{ cm}^{-1}$. Addition of 1% and 2% sodium to the 10% $\text{Re}_2\text{O}_7/\text{TiO}_2$ sample shifts the peak to $\sim 971\text{ cm}^{-1}$. Further addition of sodium, about 3%, shifts the 971 cm^{-1} peak to 961 cm^{-1} and a broad shoulder appears at $\sim 900\text{ cm}^{-1}$. The Raman spectra of the above samples under dehydrated conditions are shown in Fig.3.19. The 1005 cm^{-1} band of the 10% $\text{Re}_2\text{O}_7/\text{TiO}_2$ sample is shifted to lower wavenumbers with the addition of 1%, 2% and 3% sodium from 1005 cm^{-1} to 989, 980 and 975 cm^{-1} , respectively. A broad shoulder at $\sim 900\text{ cm}^{-1}$ which is observed in the ambient spectra of 3% $\text{Na}_2\text{O}/10\%\text{Re}_2\text{O}_7/\text{TiO}_2$ catalyst is also present here.

Comparison of the spectra also show that the Raman bands of the sodium doped samples under ambient conditions are different from those under dehydrated conditions. Additionally, the peak due to the rhenium oxide surface species under dehydrated conditions is at a higher wavenumber than that for the ambient conditions. The Raman spectra for each individual sodium doped $\text{Re}_2\text{O}_7/\text{TiO}_2$ catalysts under ambient and dehydrated conditions are included for convenience as Figs. 3.20, 3.21 and 3.22.

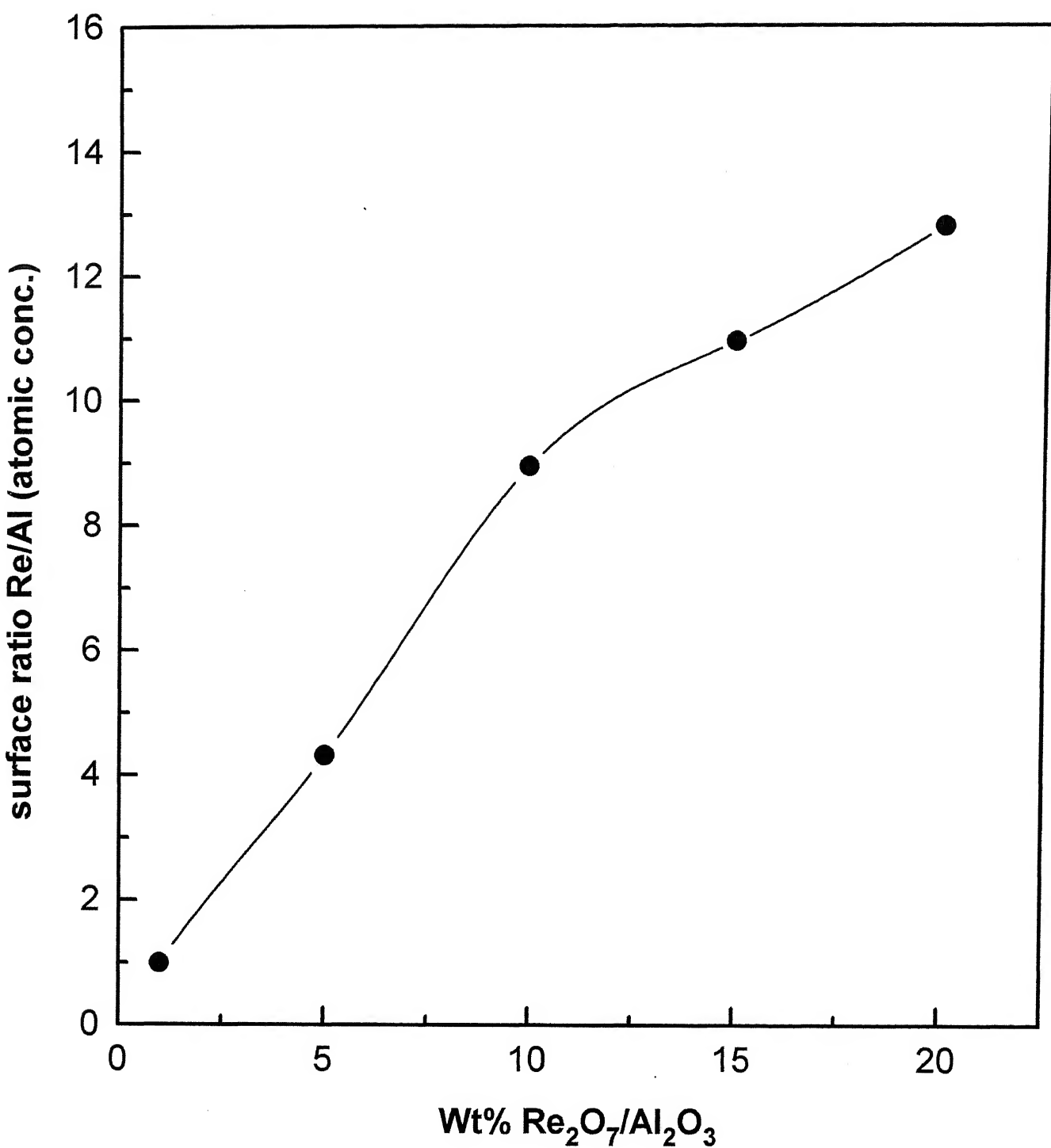


FIG. 3.1 XPS SURFACE RATIO Re/Al VERSUS WT.% Re₂O₇

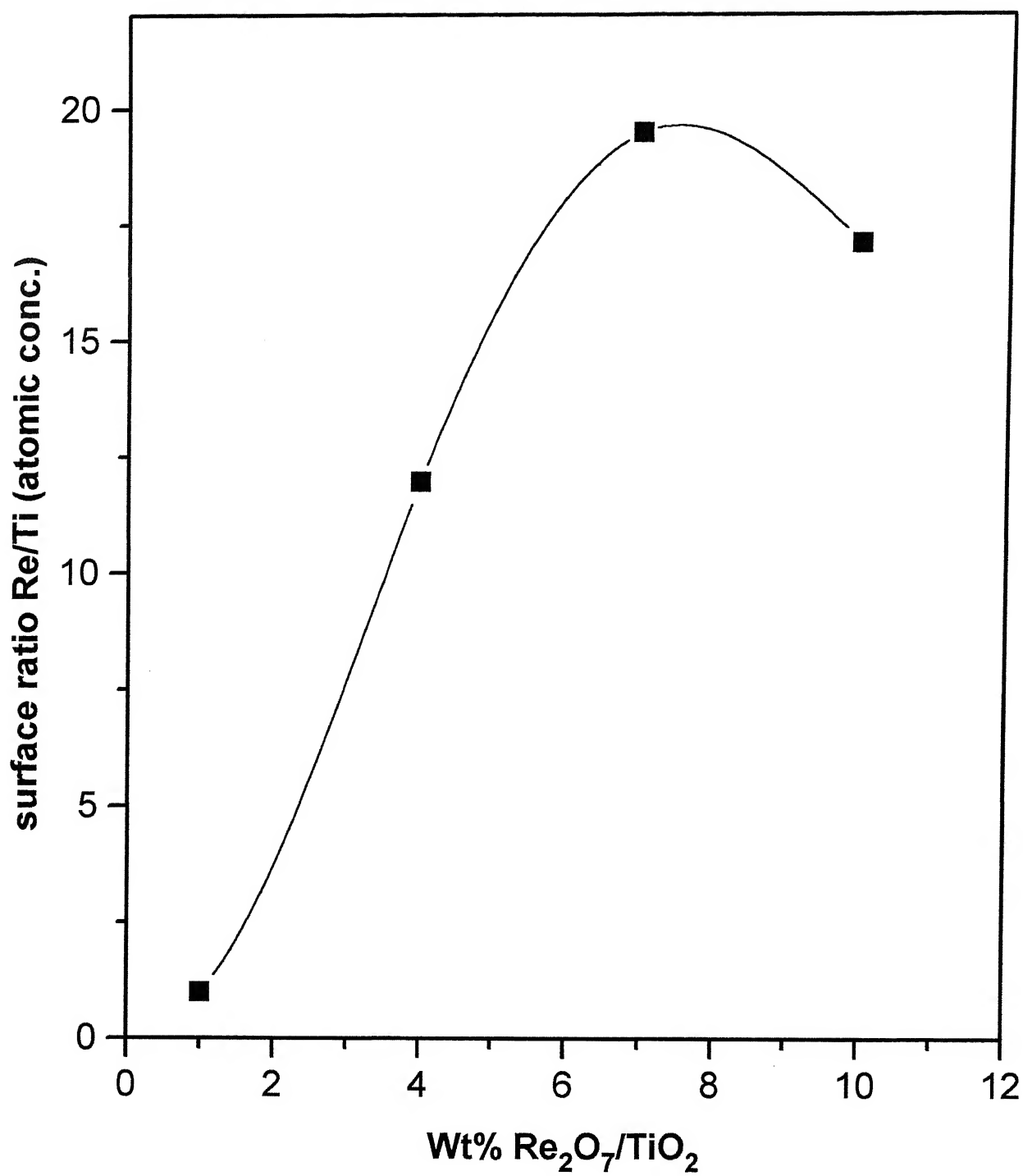


FIG. 3.2 XPS SURFACE RATIO Re/Ti VERSUS WT.% Re_2O_7

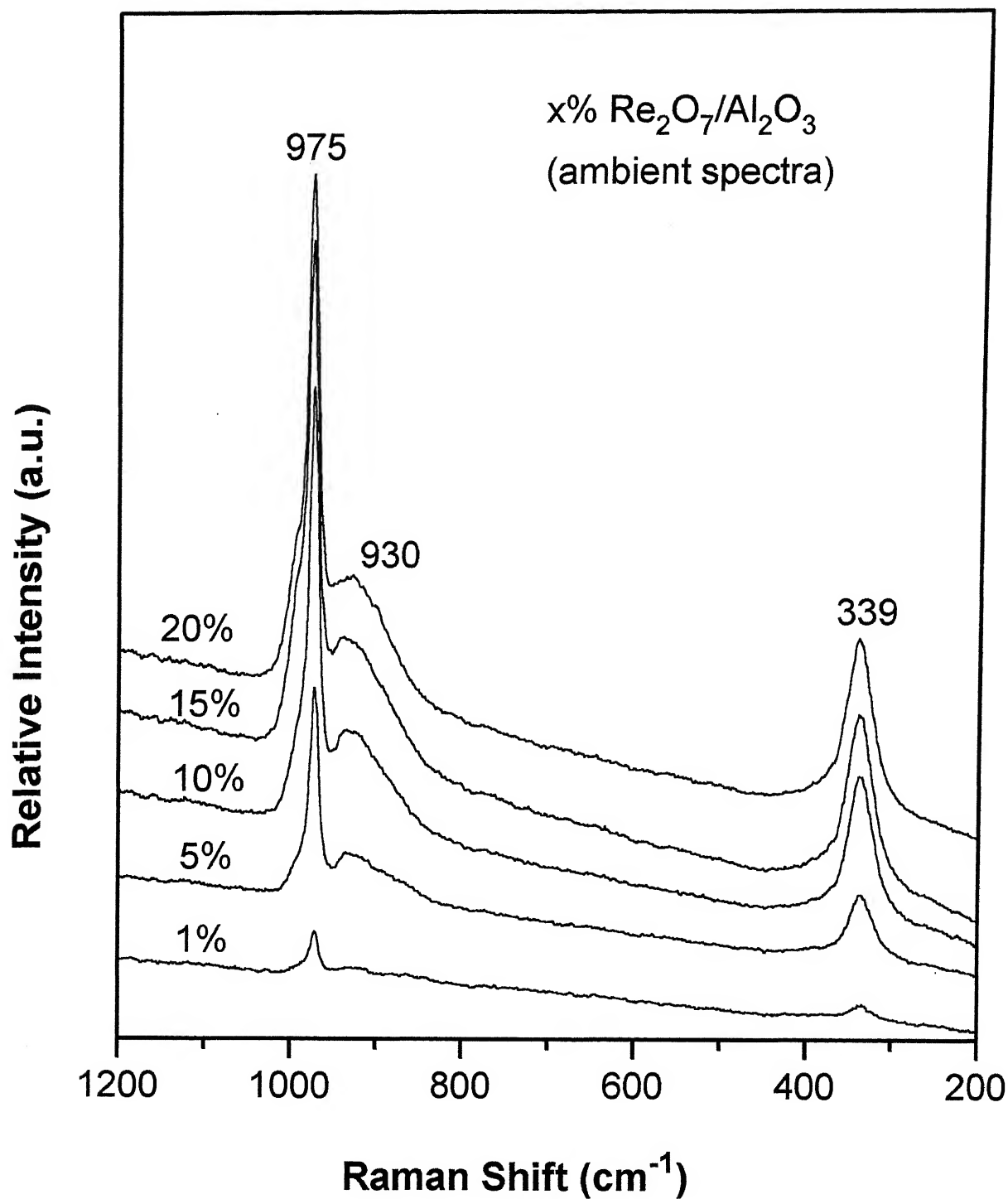


FIG. 3.3 RAMAN SPECTRA OF $\text{Re}_2\text{O}_7/\text{Al}_2\text{O}_3$ AS A FUNCTION OF Re_2O_7 LOADING. SPECTRA OBTAINED UNDER AMBIENT CONDITIONS.

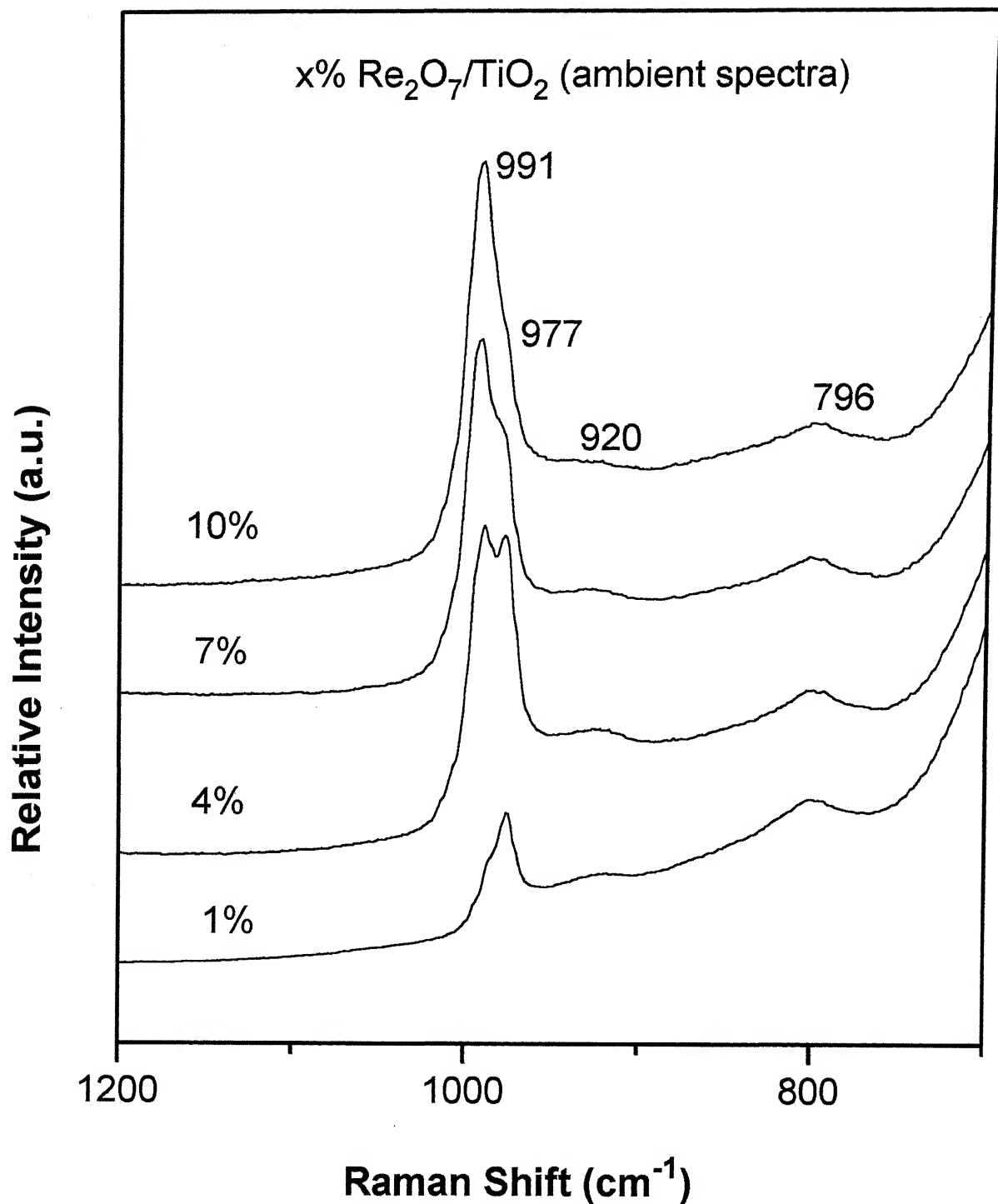


FIG. 3.4 RAMAN SPECTRA OF $\text{Re}_2\text{O}_7/\text{TiO}_2$ AS A FUNCTION OF Re_2O_7 LOADING. SPECTRA OBTAINED UNDER AMBIENT CONDITIONS

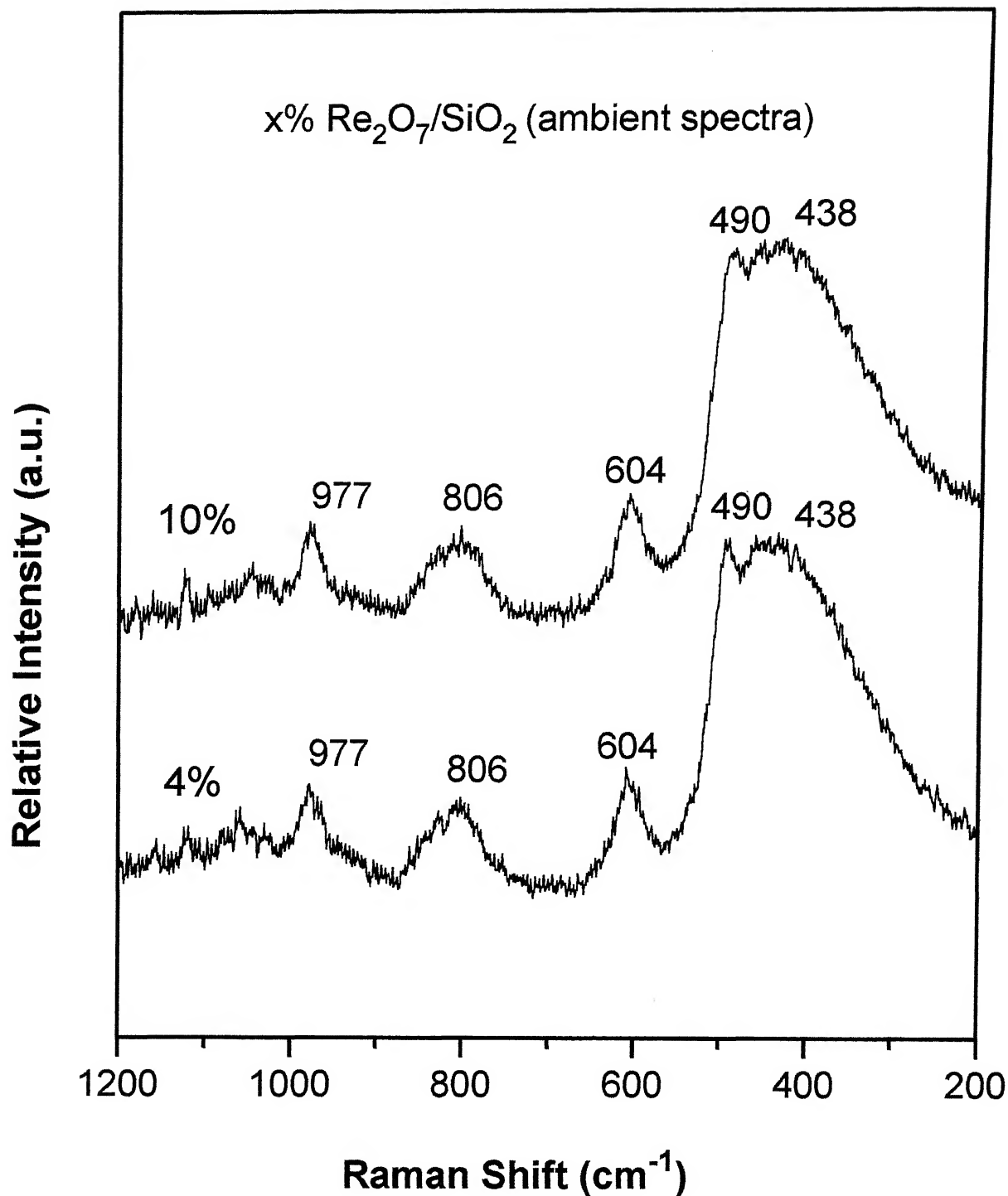


FIG. 3.5 RAMAN SPECTRA OF $\text{Re}_2\text{O}_7/\text{SiO}_2$ AS A FUNCTION OF Re_2O_7 LOADING. SPECTRA OBTAINED UNDER AMBIENT CONDITIONS.

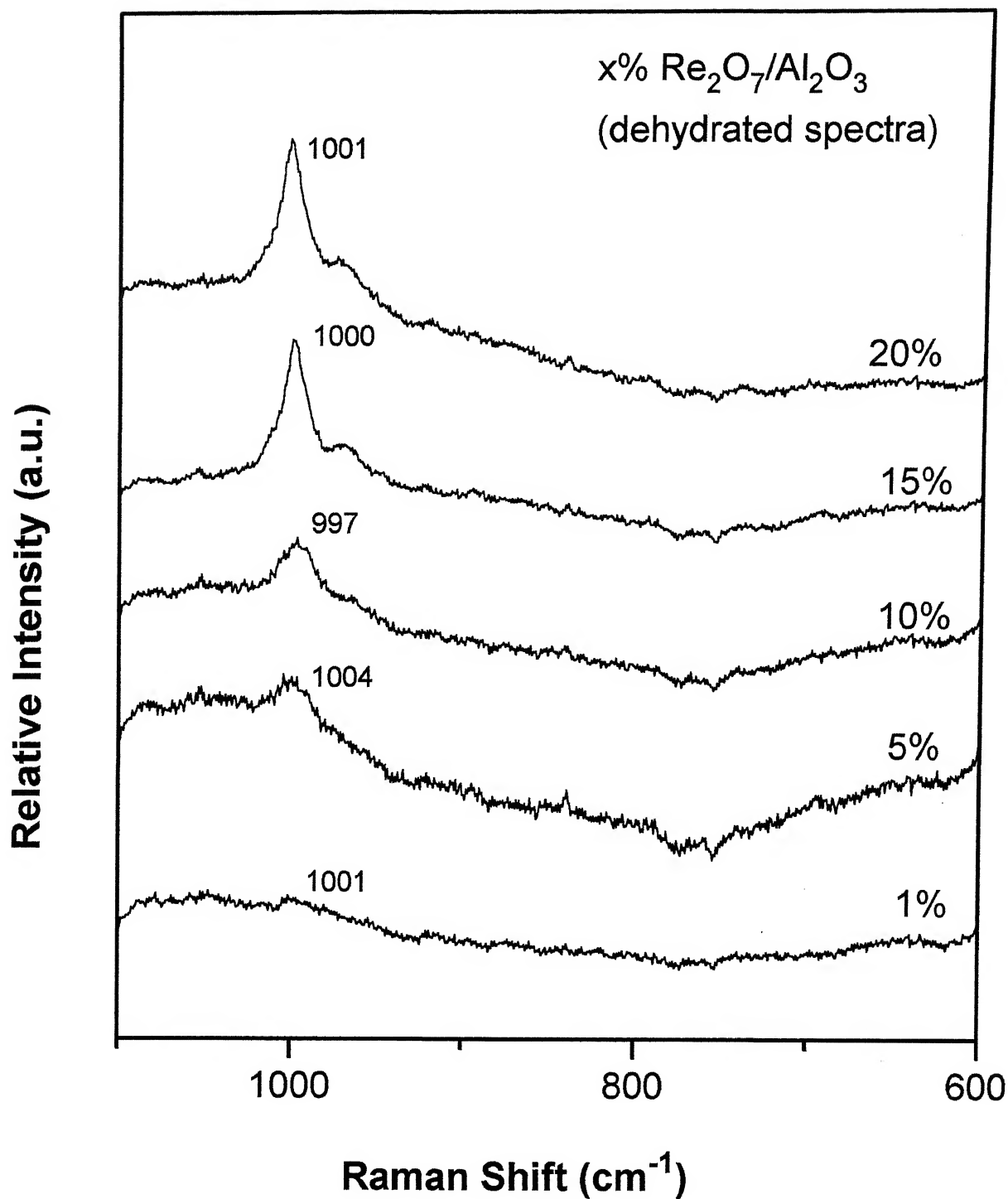


FIG. 3.6 RAMAN SPECTRA OF $\text{Re}_2\text{O}_7/\text{Al}_2\text{O}_3$ AS A FUNCTION OF Re_2O_7 LOADING. SPECTRA OBTAINED UNDER DEHYDRATED CONDITIONS.

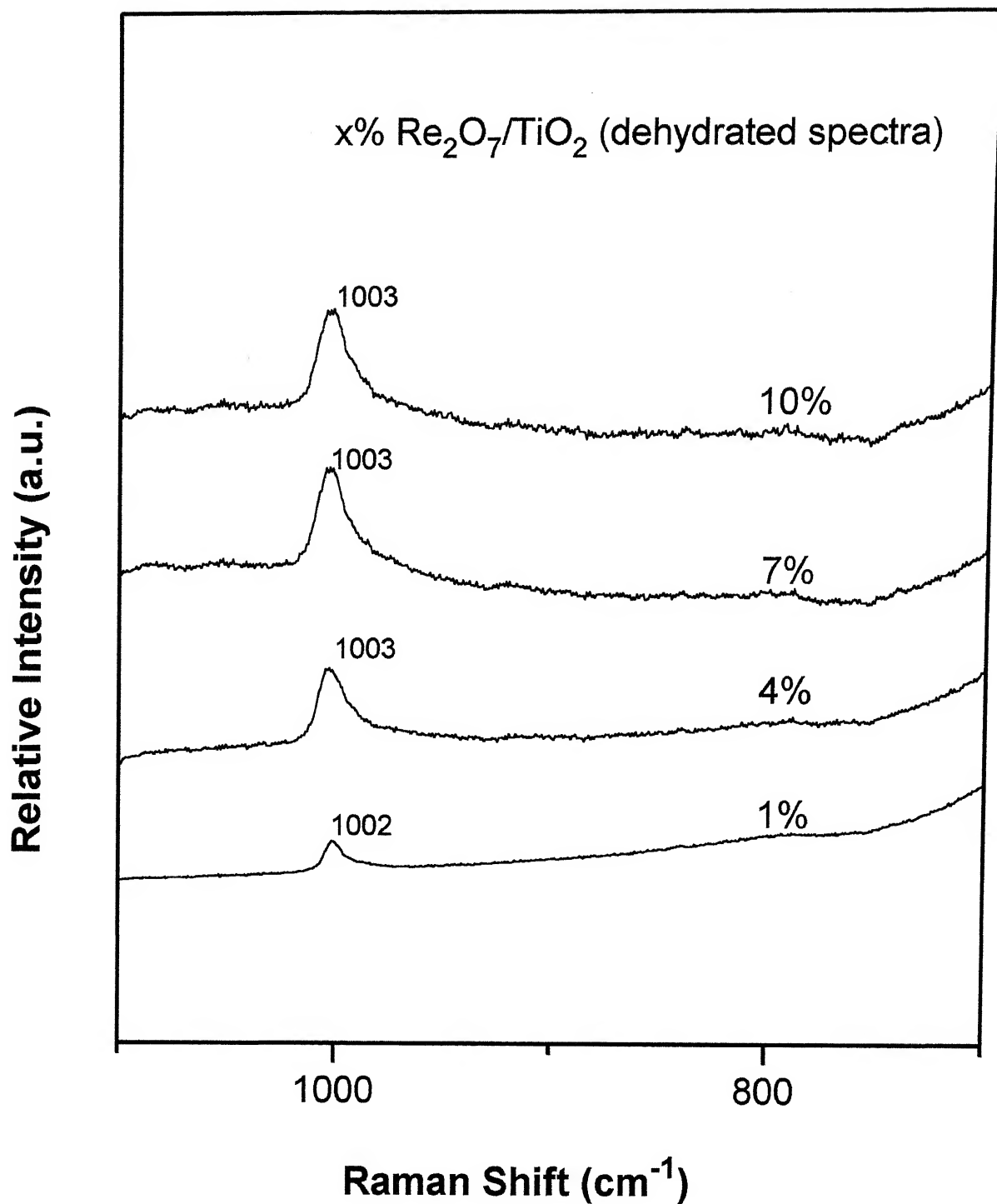


FIG. 3.7 RAMAN SPECTRA OF $\text{Re}_2\text{O}_7/\text{TiO}_2$ AS A FUNCTION OF Re_2O_7 LOADING. SPECTRA OBTAINED UNDER DEHYDRATED CONDITIONS.

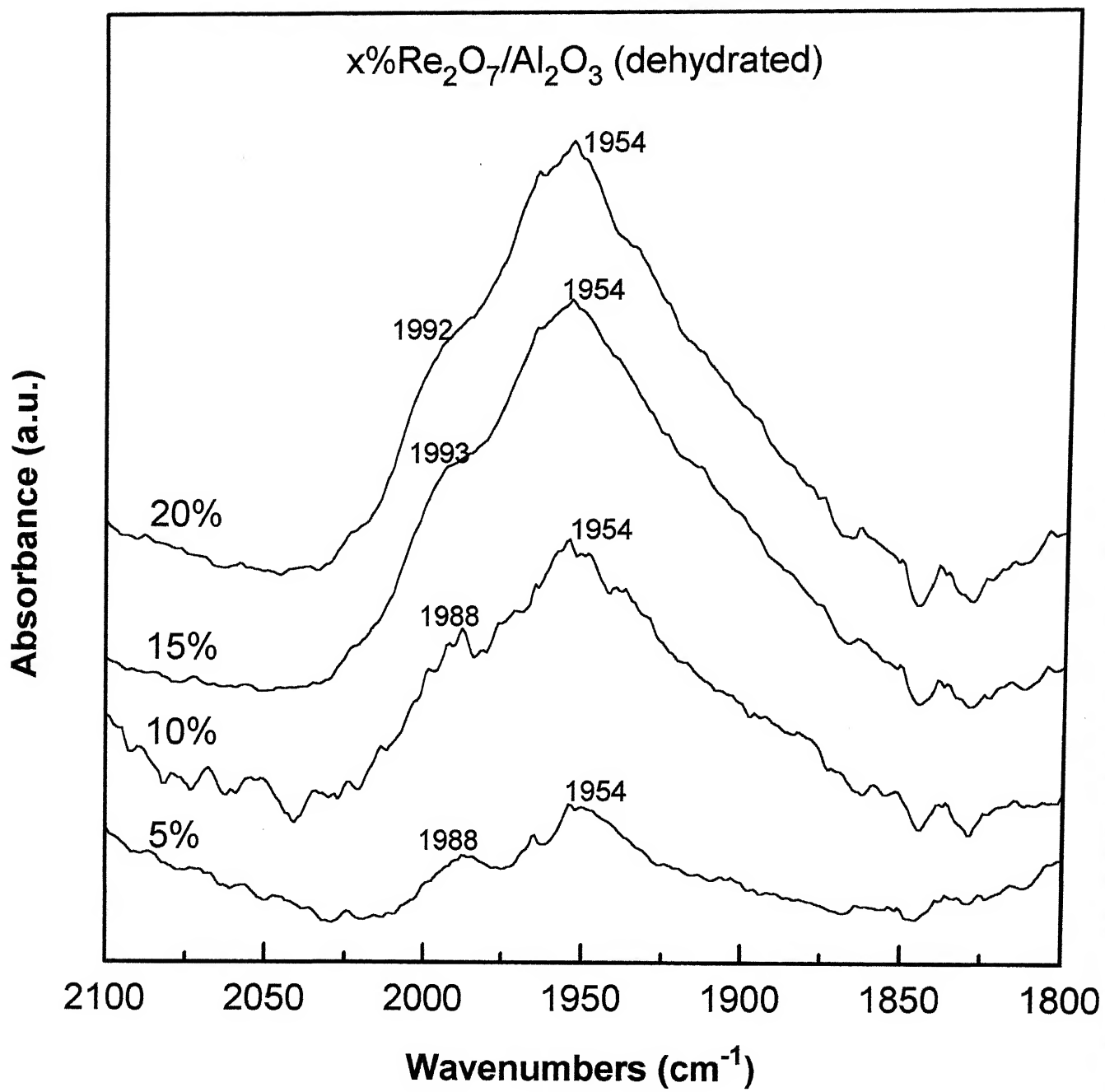


FIG. 3.8 IR SPECTRA OF $\text{Re}_2\text{O}_7/\text{Al}_2\text{O}_3$ AS A FUNCTION OF Re_2O_7 LOADING IN THE OVERTONE REGION. SPECTRA OBTAINED UNDER DEHYDRATED CONDITIONS.

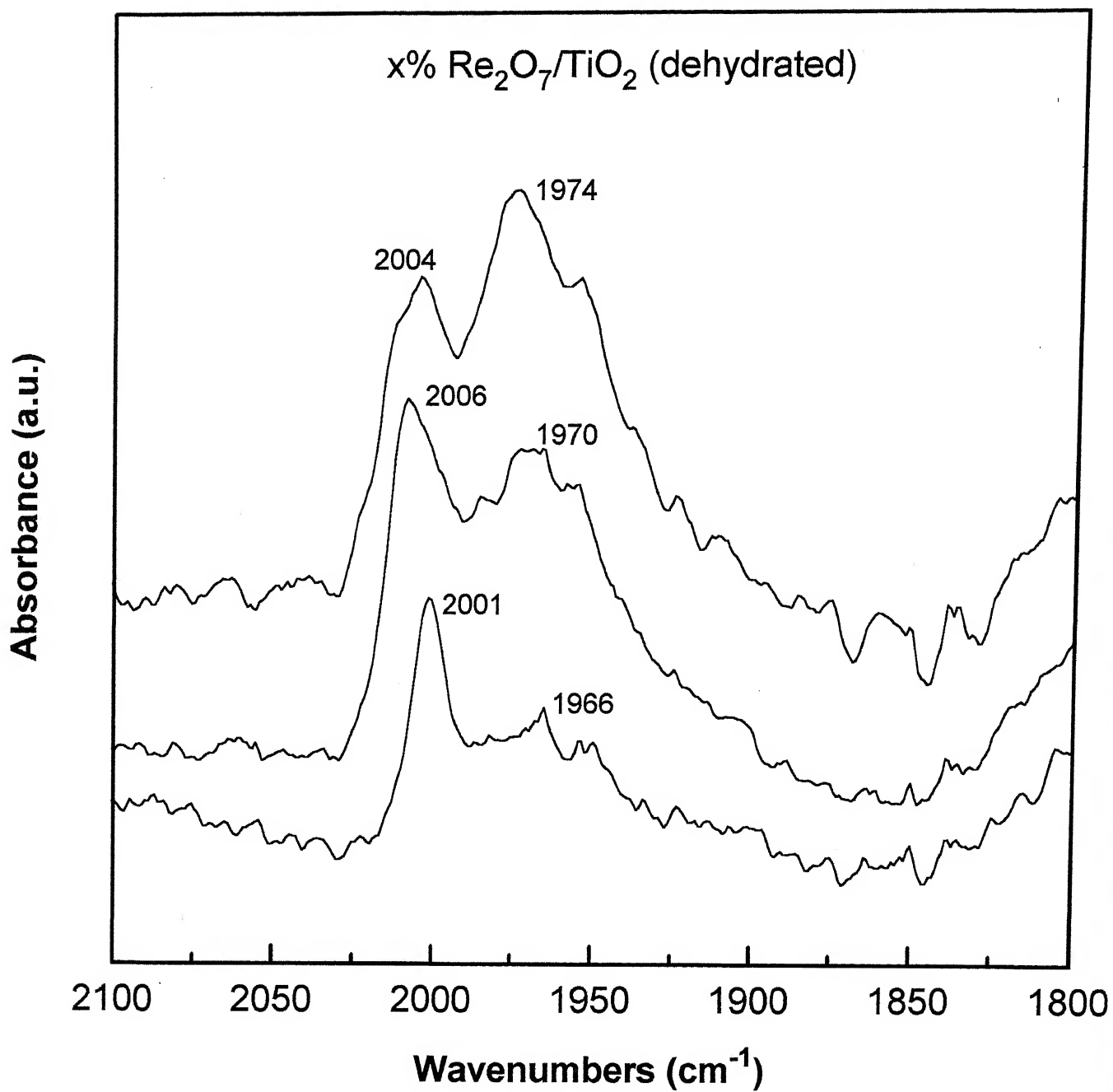


FIG. 3.9 IR SPECTRA OF Re₂O₇/TiO₂ AS A FUNCTION OF Re₂O₇ LOADING IN THE OVERTONE REGION. SPECTRA OBTAINED UNDER DEHYDRATED CONDITIONS.

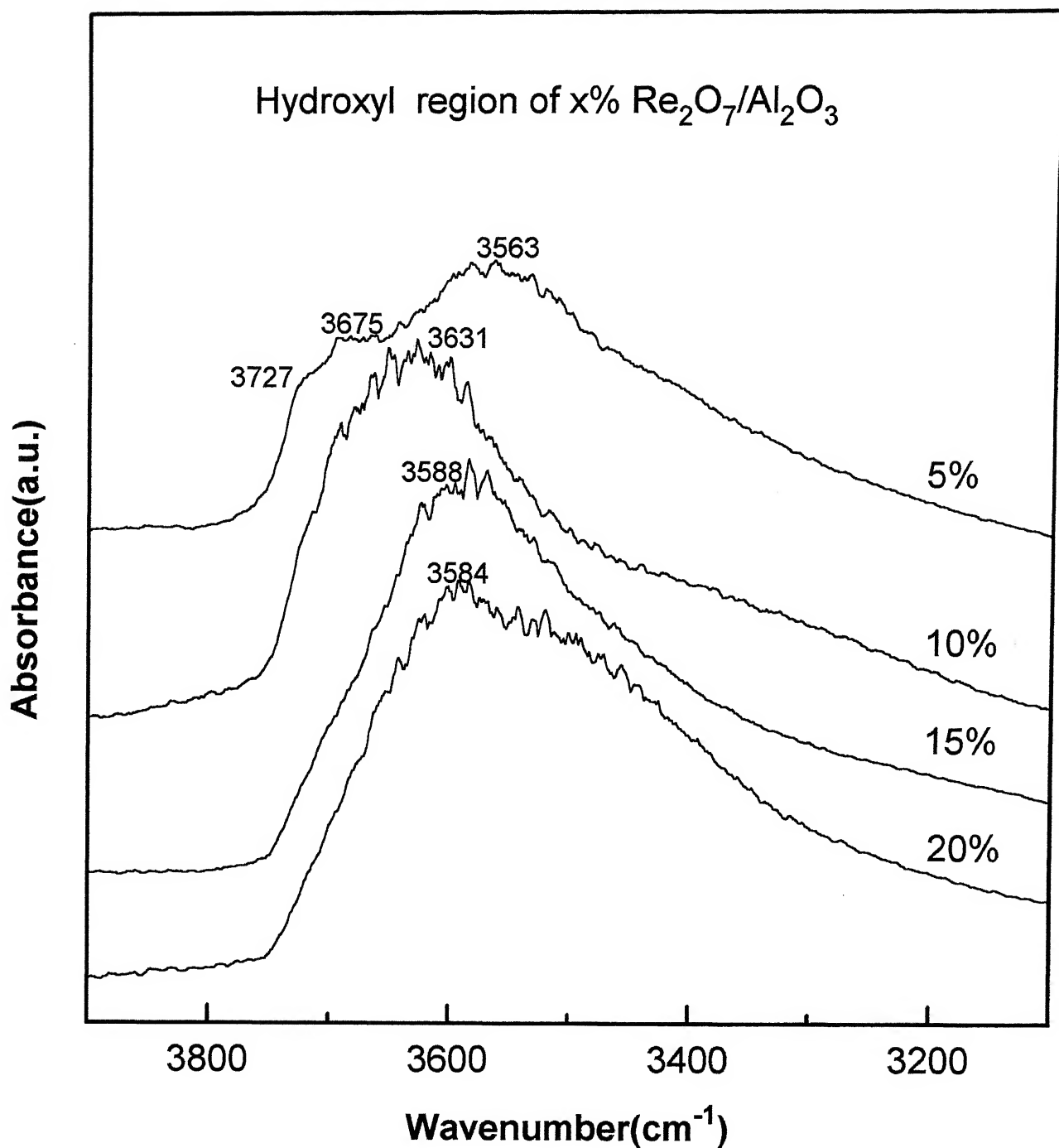


FIG. 3.10 IR SPECTRA OF $\text{Re}_2\text{O}_7/\text{Al}_2\text{O}_3$ IN THE HYDROXYL REGION AS A FUNCTION OF Re_2O_7 LOADING.

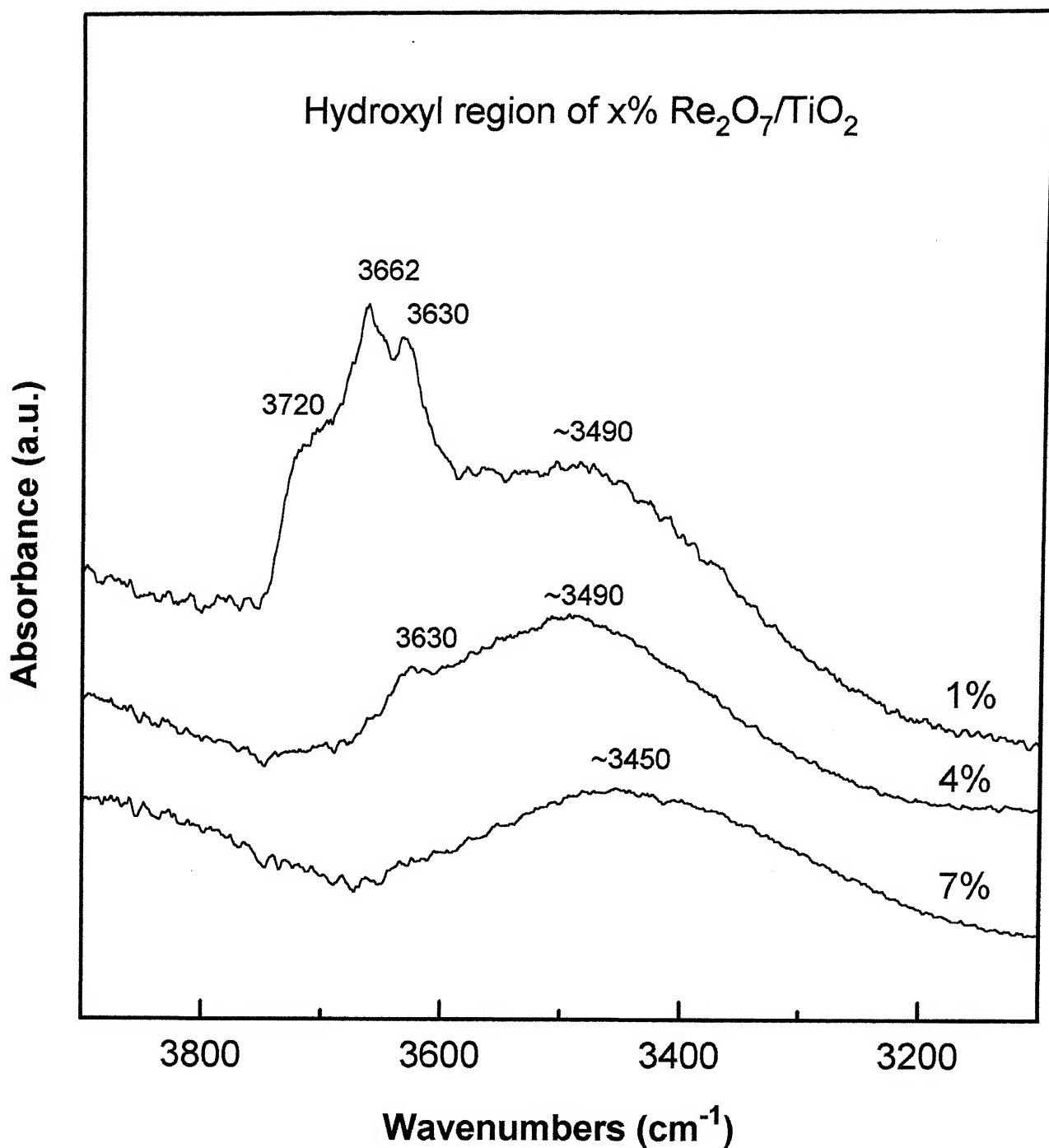


FIG. 3.11 IR SPECTRA OF $\text{Re}_2\text{O}_7/\text{TiO}_2$ IN THE HYDROXYL REGION AS A FUNCTION OF Re_2O_7 LOADING.

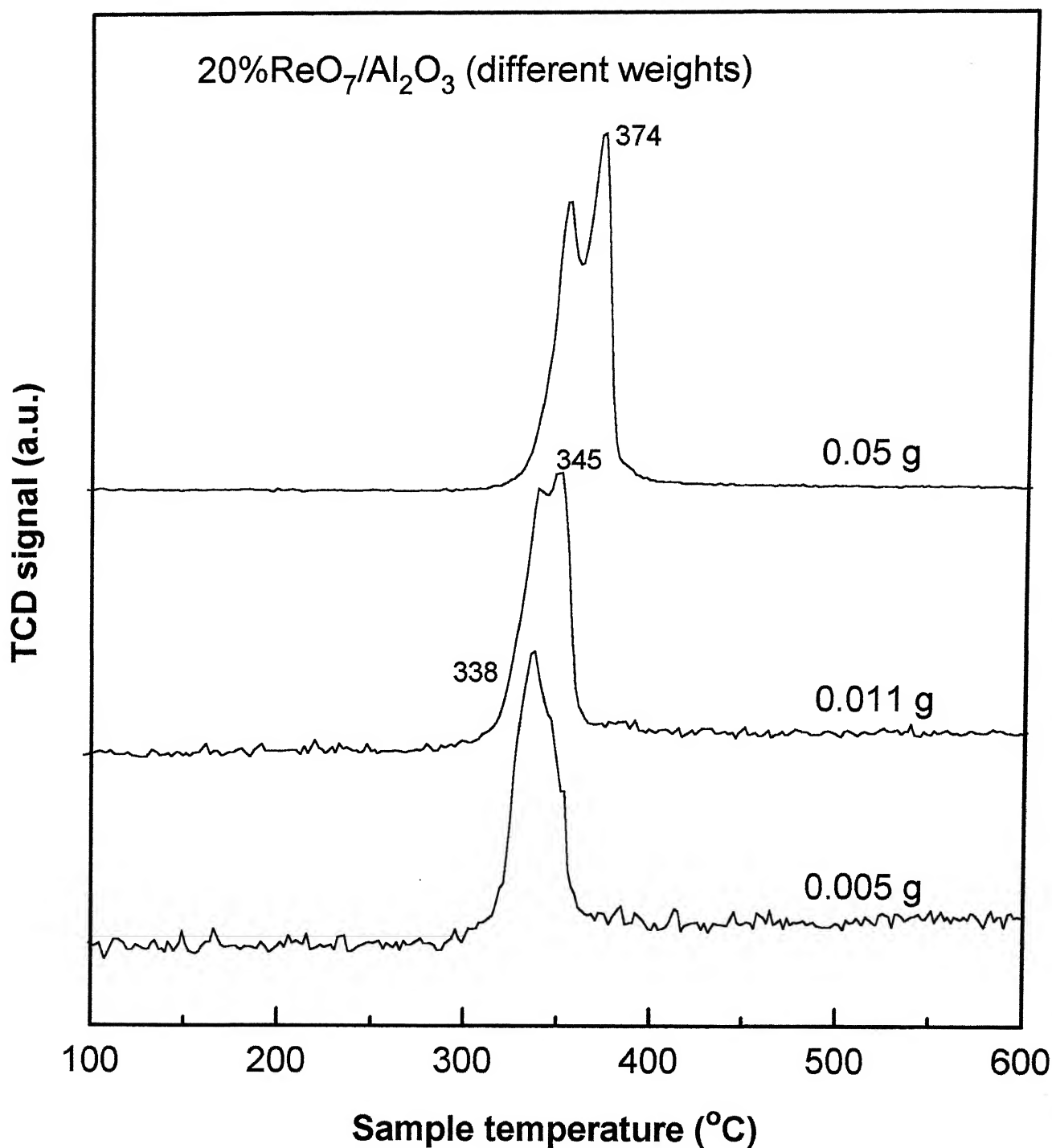


FIG. 3.12 TPR PROFILE FOR DIFFERENT WEIGHTS OF 20%Re₂O₇/Al₂O₃ CATALYST

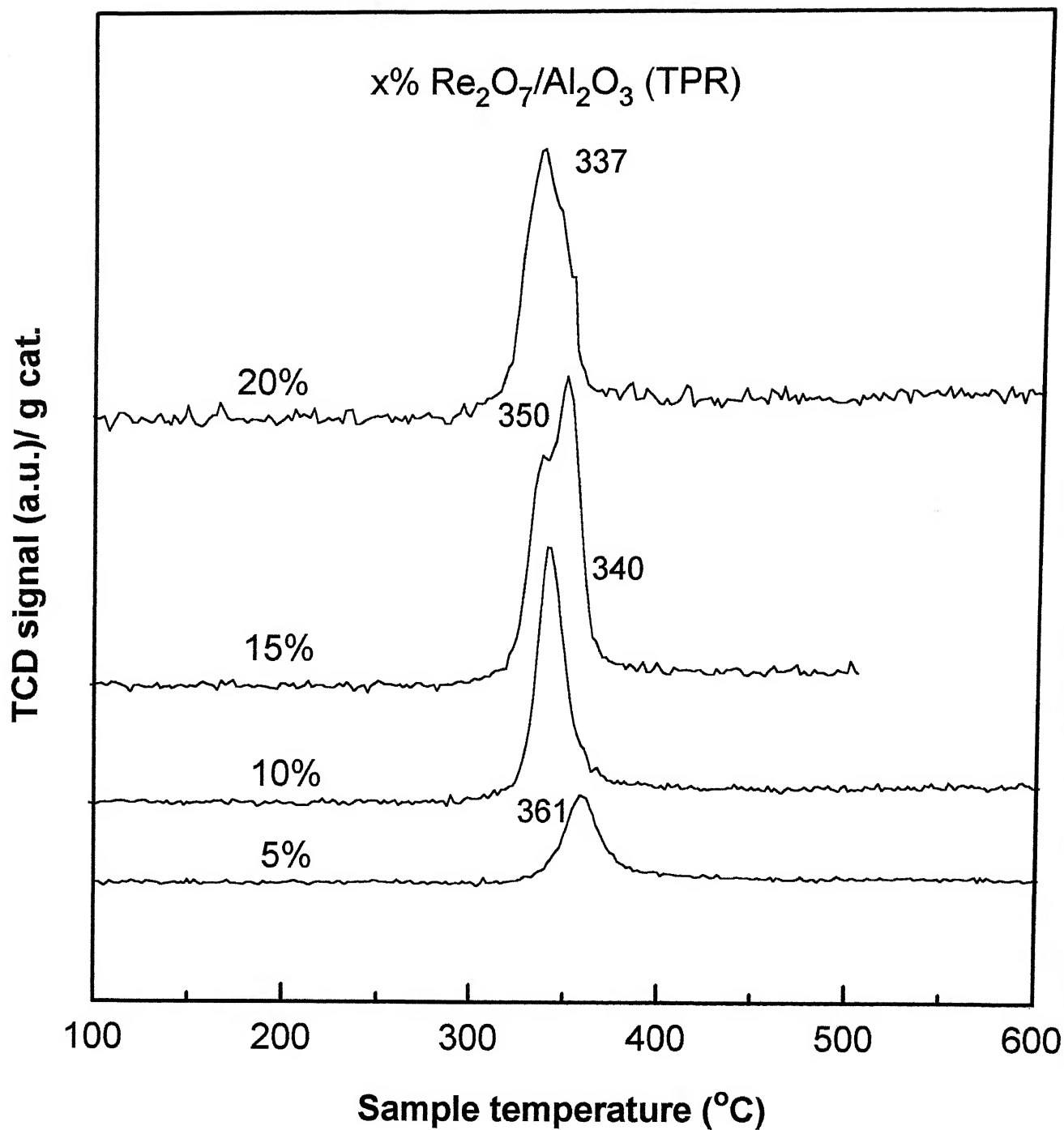


FIG. 3.13 TPR PROFILE FOR $\text{Re}_2\text{O}_7/\text{Al}_2\text{O}_3$ CATALYSTS AS A FUNCTION OF Re_2O_7 LOADING.

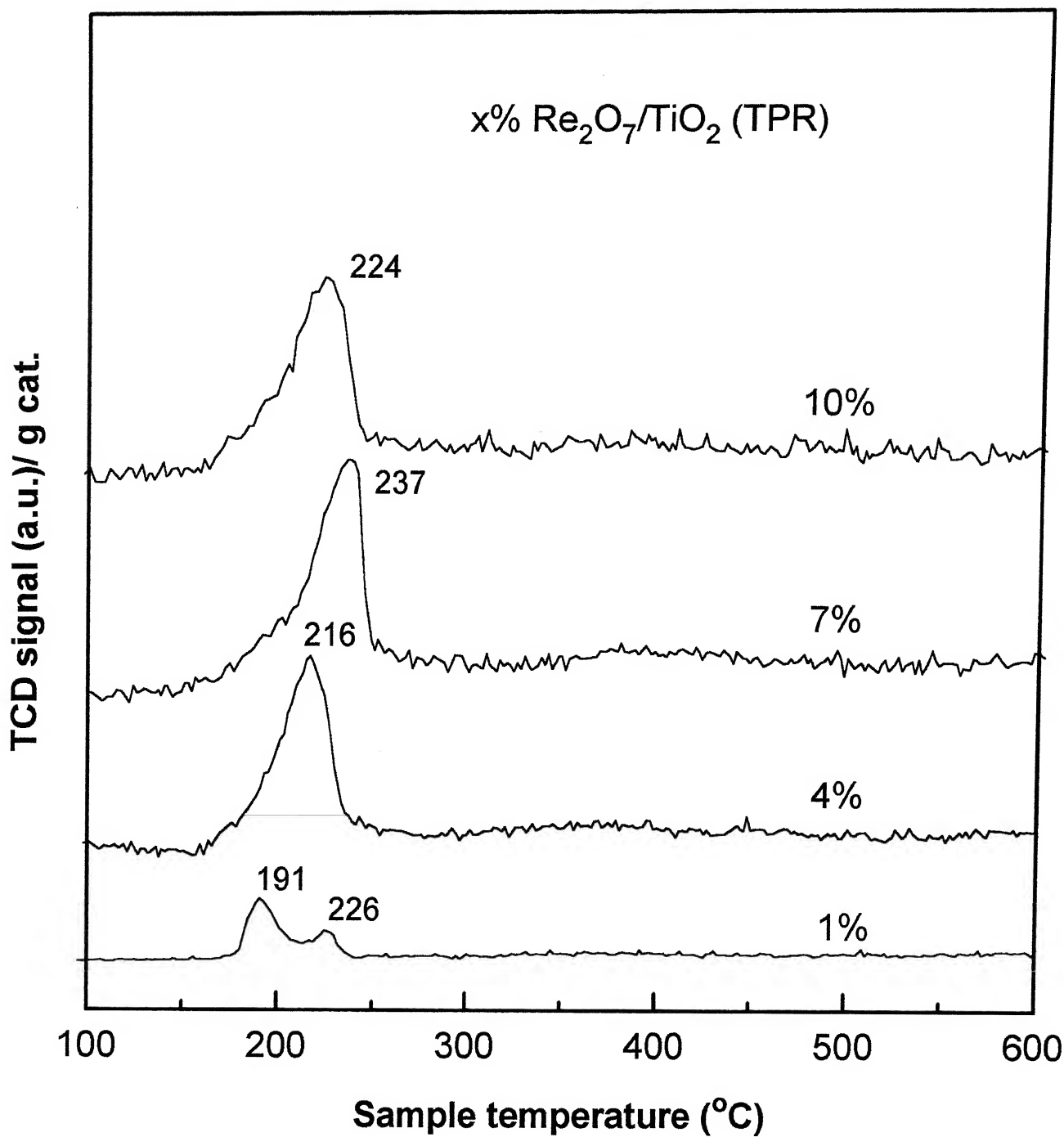


FIG. 3.14 TPR PROFILE FOR $\text{Re}_2\text{O}_7/\text{TiO}_2$ CATALYSTS AS A FUNCTION OF Re_2O_7 LOADING.

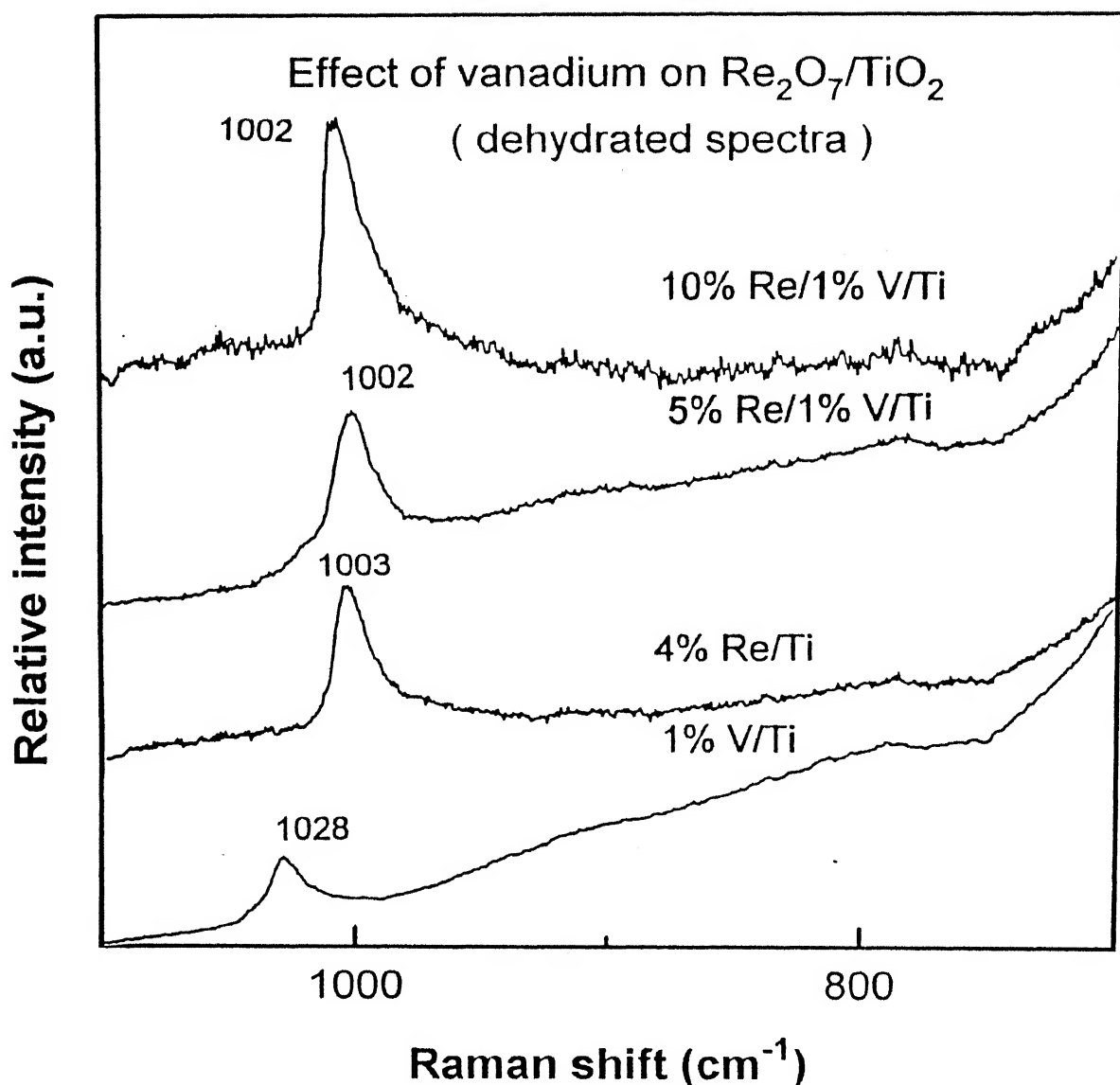


FIG. 3.15 RAMAN SPECTRA OF VANADIUM DOPED $\text{Re}_2\text{O}_7/\text{TiO}_2$ CATALYSTS UNDER DEHYDRATED CONDITIONS. THE ACTUAL LEGENDS OF EACH SPECTRUM SHOULD READ (FROM TOP TO BOTTOM) :

- | | |
|----------------------------------------------------------------------|---------------------------------------------------------------------|
| (a) $10\%\text{Re}_2\text{O}_7/1\%\text{V}_2\text{O}_5/\text{TiO}_2$ | (b) $5\%\text{Re}_2\text{O}_7/1\%\text{V}_2\text{O}_5/\text{TiO}_2$ |
| (c) $4\%\text{Re}_2\text{O}_7/\text{TiO}_2$ | (d) $1\%\text{V}_2\text{O}_5/\text{TiO}_2$ |

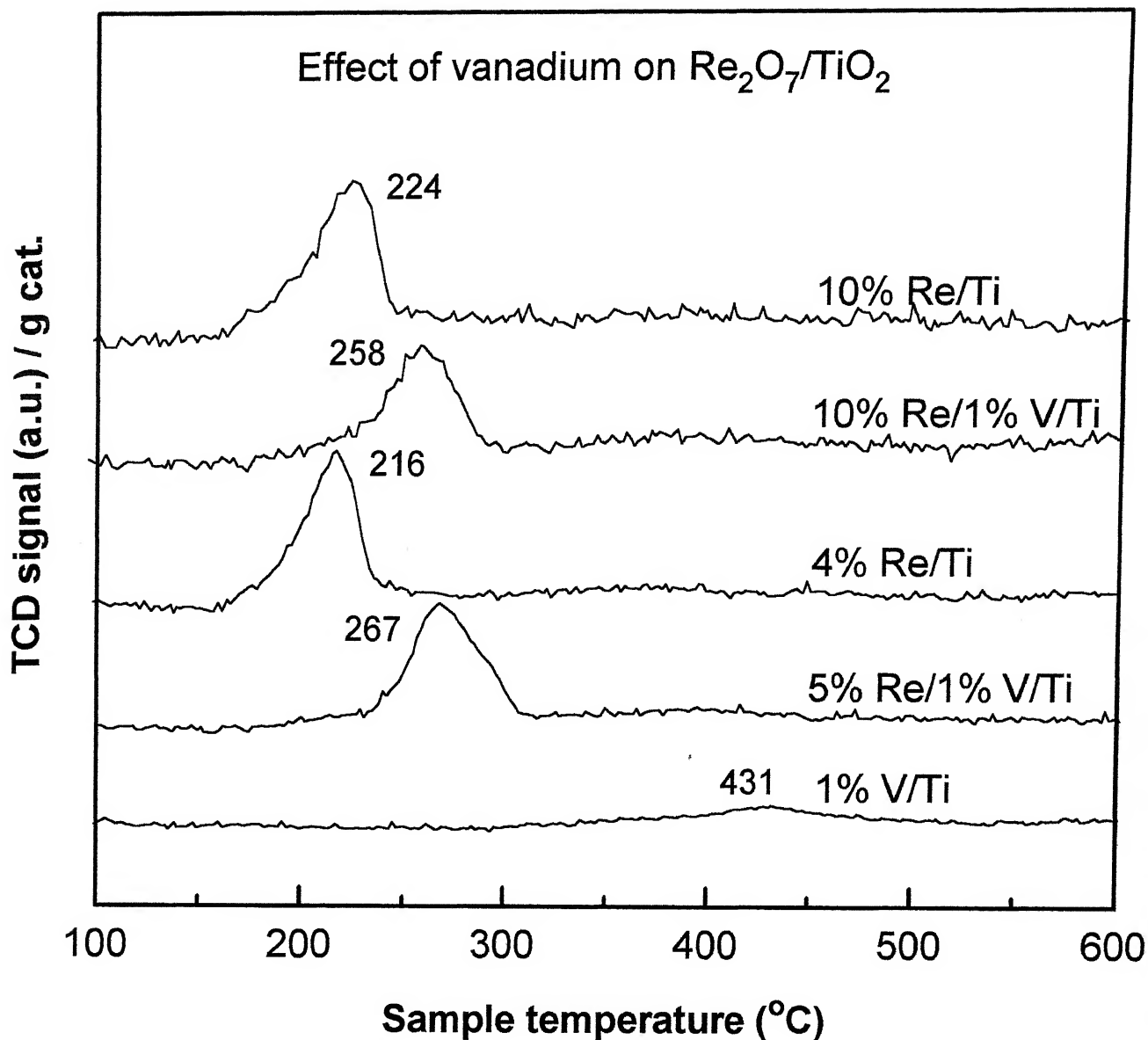


FIG. 3.16 TPR PROFILE FOR VANADIUM DOPED $\text{Re}_2\text{O}_7/\text{TiO}_2$ CATALYSTS.

THE ACTUAL LEGENDS OF EACH SPECTRUM SHOULD READ

(FROM TOP TO BOTTOM): (a) $10\%\text{Re}_2\text{O}_7/\text{TiO}_2$

(b) $10\%\text{Re}_2\text{O}_7/1\%\text{V}_2\text{O}_5/\text{TiO}_2$ (c) $4\%\text{Re}_2\text{O}_7/\text{TiO}_2$

(d) $5\%\text{Re}_2\text{O}_7/1\%\text{V}_2\text{O}_5/\text{TiO}_2$ (e) $1\%\text{V}_2\text{O}_5/\text{TiO}_2$

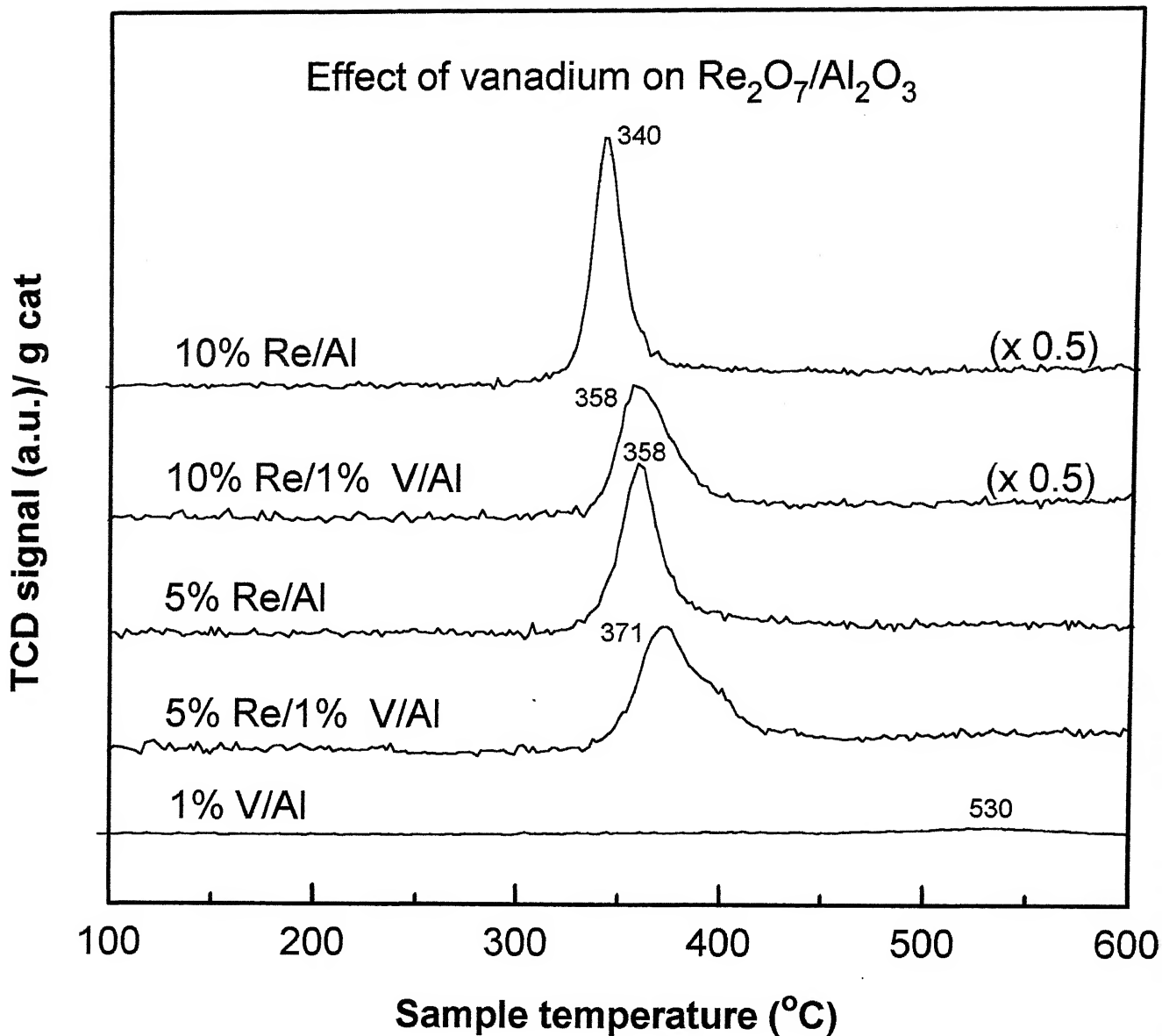


FIG. 3.17 TPR PROFILE FOR VANADIUM DOPED $\text{Re}_2\text{O}_7/\text{Al}_2\text{O}_3$ CATALYSTS.

THE ACTUAL LEGENDS OF EACH SPECTRUM SHOULD READ

(FROM TOP TO BOTTOM): (a) $10\%\text{Re}_2\text{O}_7/\text{Al}_2\text{O}_3$

(b) $10\%\text{Re}_2\text{O}_7/1\%\text{V}_2\text{O}_5/\text{Al}_2\text{O}_3$ (c) $5\%\text{Re}_2\text{O}_7/\text{Al}_2\text{O}_3$

(d) $5\%\text{Re}_2\text{O}_7/1\%\text{V}_2\text{O}_5/\text{Al}_2\text{O}_3$ (e) $1\%\text{V}_2\text{O}_5/\text{Al}_2\text{O}_3$

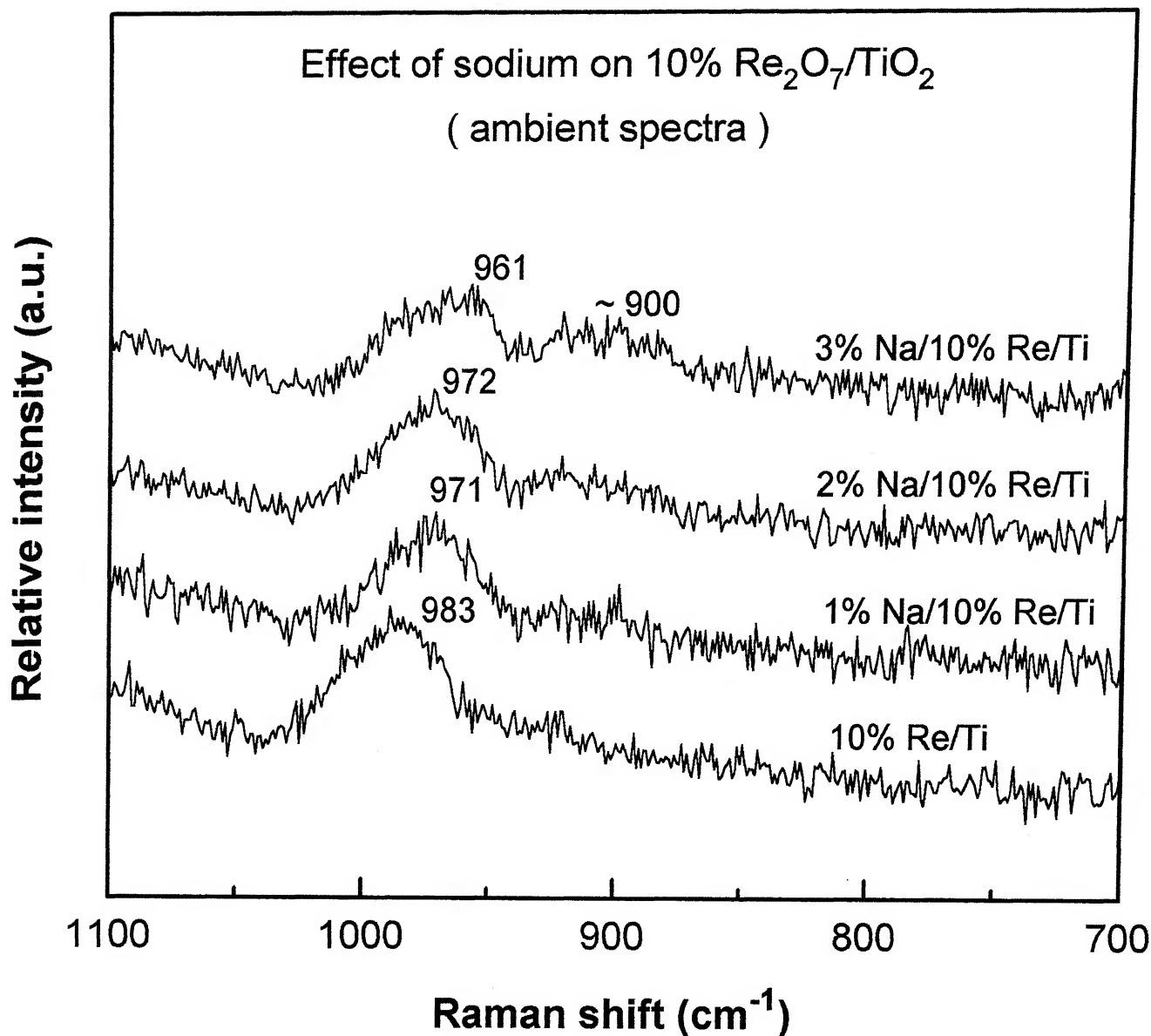


FIG. 3.18 RAMAN SPECTRA OF SODIUM DOPED $\text{Re}_2\text{O}_7/\text{TiO}_2$ CATALYSTS UNDER AMBIENT CONDITIONS. THE ACTUAL LEGENDS OF EACH SPECTRUM SHOULD READ (FROM TOP TO BOTTOM) :

- | | |
|---------------------------------------------------------------------|---------------------------------------------------------------------|
| (a) 3% $\text{Na}_2\text{O}/10\%\text{Re}_2\text{O}_7/\text{TiO}_2$ | (b) 2% $\text{Na}_2\text{O}/10\%\text{Re}_2\text{O}_7/\text{TiO}_2$ |
| (c) 1% $\text{Na}_2\text{O}/10\%\text{Re}_2\text{O}_7/\text{TiO}_2$ | (d) 10% $\text{Re}_2\text{O}_7/\text{TiO}_2$ |

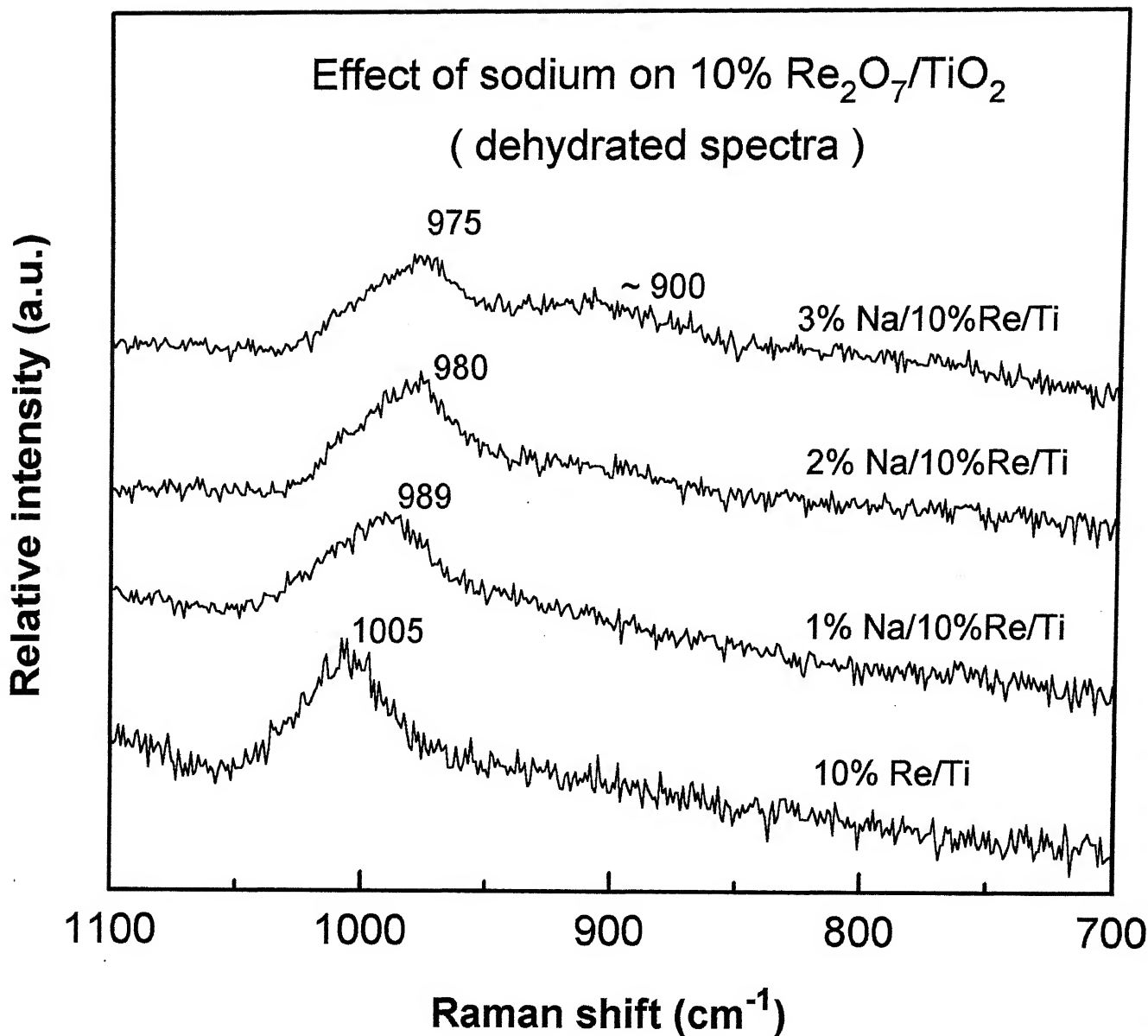


FIG. 3.19 RAMAN SPECTRA OF SODIUM DOPED $\text{Re}_2\text{O}_7/\text{TiO}_2$ CATALYSTS UNDER DEHYDRATED CONDITIONS. THE ACTUAL LEGENDS OF EACH SPECTRUM SHOULD READ (FROM TOP TO BOTTOM) :

- | | |
|---------------------------------------------------------------------|---------------------------------------------------------------------|
| (a) $3\%\text{Na}_2\text{O}/10\%\text{Re}_2\text{O}_7/\text{TiO}_2$ | (b) $2\%\text{Na}_2\text{O}/10\%\text{Re}_2\text{O}_7/\text{TiO}_2$ |
| (c) $1\%\text{Na}_2\text{O}/10\%\text{Re}_2\text{O}_7/\text{TiO}_2$ | (d) $10\%\text{Re}_2\text{O}_7/\text{TiO}_2$ |

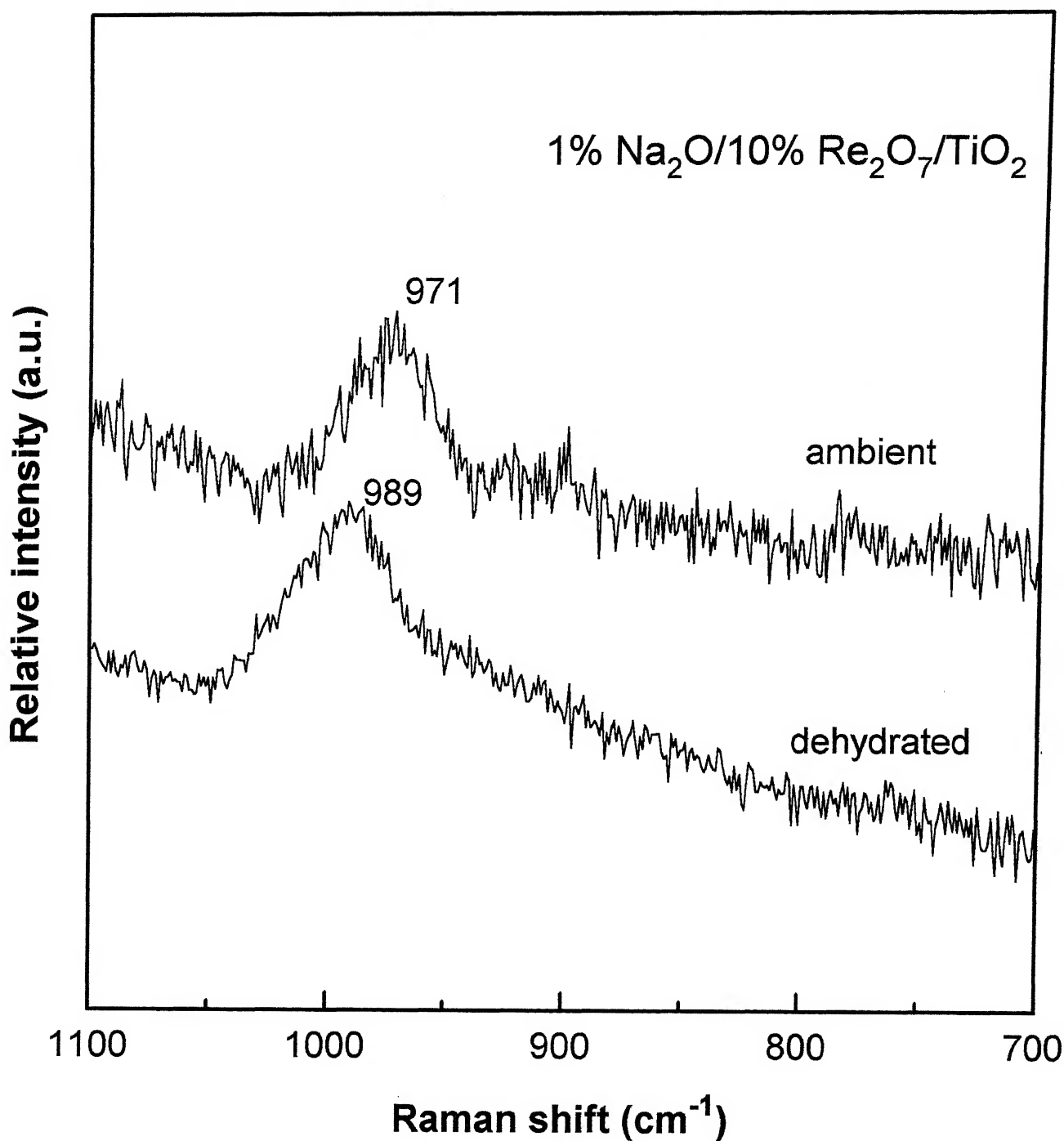


FIG. 3.20 RAMAN SPECTRA OF 1%Na₂O/10%Re₂O₇/TiO₂ CATALYSTS UNDER AMBIENT AND DEHYDRATED CONDITIONS.

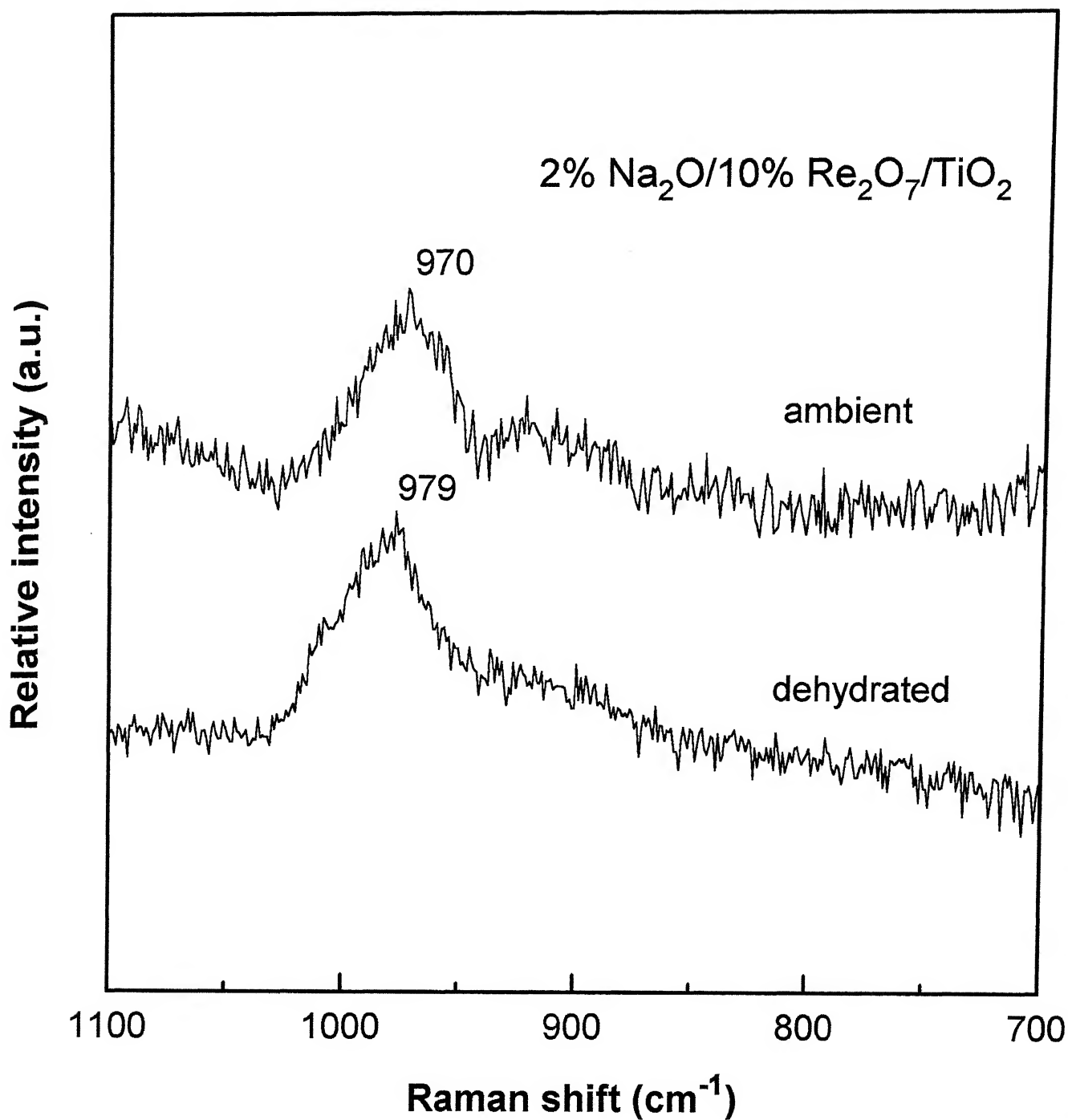


FIG. 3.21 RAMAN SPECTRA OF 2%Na₂O/10%Re₂O₇/TiO₂ CATALYSTS UNDER AMBIENT AND DEHYDRATED CONDITIONS.

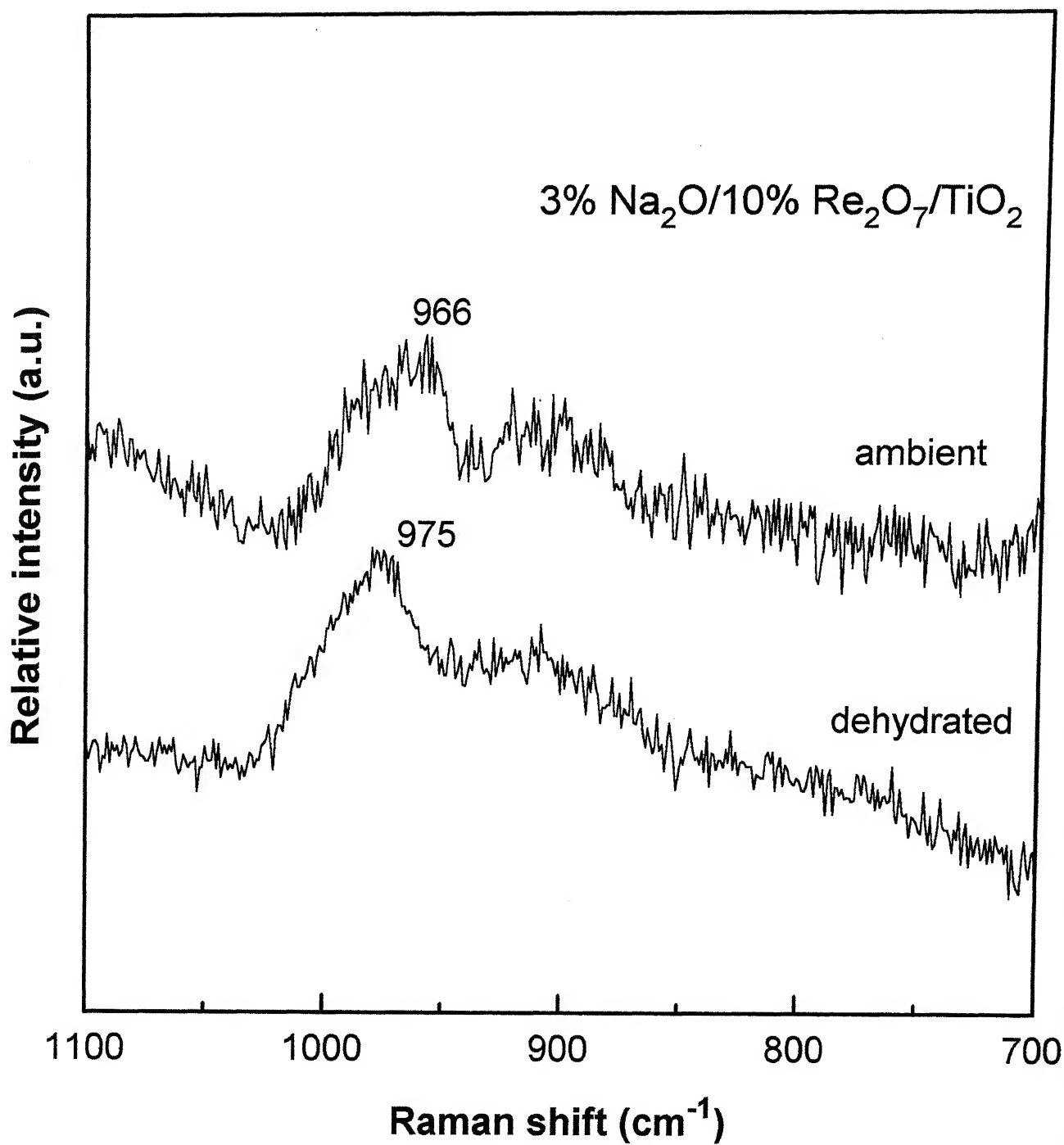


FIG. 3.22 RAMAN SPECTRA OF 3%Na₂O/10%Re₂O₇/TiO₂ CATALYSTS UNDER AMBIENT AND DEHYDRATED CONDITIONS.

TABLE 3.1 ATTEMPTED CONCENTRATION OF RHENIUM ON
DIFFERENT OXIDE SUPPORTS

Oxide Support	Attempted Re_2O_7 loading (wt. %)	Attempted rhenium conc. (atoms/nm ²)
Al_2O_3	1	0.14
	5	0.73
	10	1.54
	15	2.44
	20	3.45
TiO_2	1	0.46
	4	1.88
	7	3.40
	10	5.02
SiO_2	1	0.08
	4	0.35
	10	0.92

TABLE 3.2 ATOMIC CONCENTRATIONS OF RHENIUM AND ADDITIVES IN
DIFFERENT DOPED SUPPORTED RHENIA CATALYSTS

Class of catalyst	Re ₂ O ₇ loading in catalyst (wt.%)	Rhenium conc. in catalyst (atoms/nm ²)	Additive loading in catalyst (wt.%)		Additive conc. in catalyst (atoms/nm ²)	Rhenium to Additive ratio
			Vanadium	Sodium		
Re-V-Ti	5	2.36	1	—	1.22	1.93
	10	4.97	1	—	1.22	4.07
Re-V-Al	5	0.72	1	—	0.37	1.95
	10	1.52	1	—	0.37	4.11
Re-Na-Ti	10	5.02	—	1	3.21	1.56
	10	5.02	—	2	6.49	0.77
	10	5.02	—	3	9.83	0.50

CENTRAL LIBRARY
UTTAR PRADESH
No. A 125022

TABLE 3.3 HYDROGEN CONSUMED BY DIFFERENT SUPPORTED RHENIA CATALYSTS DURING TPR MEASUREMENTS

Catalyst	Rhenium loading (wt.%)	Hydrogen consumed ($\mu\text{moles/g}$)	Atoms of hydrogen (/g)	Atoms of rhenium (/g)	Hydrogen to rhenium ratio
$\text{Re}_2\text{O}_7/\text{Al}_2\text{O}_3$	5	566.6	6.83×10^{20}	1.31×10^{20}	5.21
	5	524.7	6.32×10^{20}	1.31×10^{20}	4.83
	10	1297.8	15.66×10^{20}	2.76×10^{20}	5.66
	10	1511.5	18.21×10^{20}	2.76×10^{20}	6.59
	15	2057.9	24.79×10^{20}	4.39×10^{20}	5.65
	15	1708.8	20.58×10^{20}	4.39×10^{20}	4.69
	20	1906.2	22.96×10^{20}	6.22×10^{20}	3.69
	20	1867.5	22.50×10^{20}	6.22×10^{20}	3.62
	20	2368.2	28.53×10^{20}	6.22×10^{20}	4.59
$\text{Re}_2\text{O}_7/\text{TiO}_2$	1	101.7	1.26×10^{20}	2.51×10^{19}	4.88
	1	114.1	1.37×10^{20}	2.51×10^{19}	5.47
	4	420.9	5.07×10^{20}	1.04×10^{20}	4.89
	4	390.1	4.70×10^{20}	1.04×10^{20}	4.54
	7	571.8	6.89×10^{20}	1.87×10^{20}	3.68
	7	479.5	5.78×10^{20}	1.87×10^{20}	3.09
	10	430.5	6.21×10^{20}	2.76×10^{20}	2.25
	10	515.4	5.19×10^{20}	2.76×10^{20}	1.88

Chapter 4

Discussion

The surface rhenia species were studied using several characterization techniques. The combined information from the characterization techniques give a better understanding of the surface rhenia species. It is known that the surface rhenium oxide species is extremely volatile [18]. This is related to volatility of Re_2O_7 . At elevated temperatures, as soon as two surface species come in close proximity, they combine to form a gaseous Re_2O_7 molecule and desorb from the surface. The actual rhenium content on the surface is thus usually less than the attempted amount and the difference between the actual and attempted rhenia loading is more pronounced at higher loading. In this study, however, the actual rhenium content on the samples was not determined and the weight percents denote the attempted rhenia content.

4.1 XPS Studies

XPS can detect most of the surface metal oxide atoms up to monolayer coverage. The XPS signal is directly proportional to the rhenium oxide on the surface. Since the ratio of rhenium atom to titanium or aluminum atom increases with rhenia loading up to a certain limit, the species is well dispersed. This linear increase of rhenium atom to support cation atom below monolayer coverage is in accordance with the model by

Kerkeff and Moulijn [47] and is also observed for supported vanadium oxide, tungsten oxide, molybdenum oxide and chromium oxide catalysts [48]. For supported vanadium oxide, tungsten oxide, molybdenum oxide and chromium oxide catalysts the surface atom/surface cation attains a constant value above monolayer limits due to crystallite formation. A similar effect is observed for the supported rhenia samples. However, for supported rhenia samples crystallites of rhenia are never formed since at the calcination temperatures used Re_2O_7 volatilizes. In fact rhenia loss takes place at all loadings but is more pronounced at higher loadings. Thus, from the XPS surface studies it can be concluded that the surface rhenia species is well dispersed on the support surface and the rhenium content decreases at high surface coverages due to volatility of the rhenia species. The approach to constant values of the ratio of rhenium atom to support cation atom marks the monolayer limit of these supports, however, since the actual amount of rhenia is not known the true monolayer limit is not determined.

4.2 Oxide Supports and Rhenium Oxide Reference Compounds

The structure of the surface rhenium oxide species under ambient and dehydrated conditions is determined by means of Raman and Infrared studies. The assignment of the Raman bands present in the various spectra are done in relationship with reference compounds. The spectra of the oxide supports and some rhenium oxide reference compounds are discussed below.

Most of the metal oxide vibrations lie in the $100\text{-}1200\text{ cm}^{-1}$ region. Since the oxide supports are also metal oxides it is, therefore, necessary to know the Raman vibrations

of the oxide supports as well as rhenium oxide reference compounds. The Raman spectra of γ -alumina is featureless in the 100-1200 cm^{-1} region. However, TiO_2 and SiO_2 supports possess strong Raman bands in the 100-800 cm^{-1} region. The TiO_2 support has major Raman bands at 144, 199, 399, 448, 520, 643 and a weak band at 794 cm^{-1} [49]. For SiO_2 , Raman bands are present at 432, 482, 608, 802 and 972 cm^{-1} [49]. The IR bands of these oxide supports, TiO_2 , SiO_2 and Al_2O_3 are, however, very strong in this region owing to their ionic character [50].

A stick diagram of some of the rhenium oxide reference compounds is given in Fig.4.1[18,20]. The perrhenate ion in aqueous solution has a perfect ReO_4^- type tetrahedral structure with symmetric, asymmetric and bending vibrations at 971, 916 and 332 cm^{-1} respectively. For tetrahedrally coordinated molecules confined to a crystalline lattice, the symmetry is lower than tetrahedral. Solid NaReO_4 having a S_4 symmetry is such an example and possesses Raman bands at 963, 928, 890, 369 and 331 cm^{-1} . ReO_3F with a C_{3v} and ReF_3O_2 with a C_{2v} symmetry are four and five coordinated rhenium oxide compounds possessing Raman bands at 1009, 980, 403, 321 cm^{-1} and 1026, 990, 370 cm^{-1} , respectively. $\alpha\text{-Li}_6\text{ReO}_6$ has an ideal ReO_6 type octahedral structure with three of the fundamental modes active at 680, 505 and 360 cm^{-1} .

4.3 Ambient Conditions

The Raman spectra of rhenium oxide on TiO_2 and Al_2O_3 supports under ambient conditions show the presence of only one type of rhenium oxide species irrespective of the rhenia loading. Comparison of the band positions with the rhenia reference

compounds suggest that the surface rhenia species on the alumina and titania supports closely resemble that of a tetrahedral ReO_4^- species in aqueous solution (971 cm^{-1} , symmetric stretching mode; 916 cm^{-1} asymmetric stretching mode; 332 cm^{-1} , bending mode) [22]. Furthermore, the spectra does not show any bands in the $800, 450$ and 200 cm^{-1} region which are characteristic of the Re-O-Re linkages. Absence of these bands show that the rhenium oxide species on the surface is isolated.

Under ambient conditions, the surface of titania and alumina are covered by a film of water which are several monolayers thick and the metal oxide species are present in this water film [49]. According to a model proposed by Deo and Wachs [49], the surface metal oxide molecular structures under ambient conditions are dependent on the net pH at which the surface possess zero surface charge. This pH is determined by the combined pH of the oxide support and metal oxide overlayer. Independent of pH and ionic concentration, the hydrated ReO_4^- species is the only stable rhenium oxide species present in aqueous solution [51]. Thus, according to this model, the only rhenium oxide species expected on the surface under ambient conditions irrespective of loading or support is the hydrated ReO_4^- species. This agrees well with the experimental results obtained in this study for the surface rhenia species on the TiO_2 and Al_2O_3 supports since the hydrated ReO_4^- species is the only species present under ambient conditions. Thus, the surface rhenium oxide species under ambient conditions are hydrated, independent of loading and possess an isolated ReO_4^- structure.

4.4 Dehydrated conditions

Under reaction conditions, the catalyst temperature is usually several hundred degree Celsius. At temperatures greater than 250°C, the surface moisture present under ambient conditions desorbs [42] and the surface rhenia species directly anchors to the oxide support. The anchoring of the surface rhenia species is evident from the gradual depletion of the surface hydroxyl group as observed from the *in situ* IR spectra of the supported rhenia samples as a function of loading (Fig.3.10 and Fig.3.11). Thus, under dehydrated conditions, the molecular structure of the surface rhenia species is different from the ReO_4^- species present under ambient conditions.

The Raman bands at 1000 cm^{-1} (Fig. 3.6) and 1003 cm^{-1} (Fig.3.7) for the surface rhenia species on Al_2O_3 and TiO_2 , respectively, are observed to increase with Re_2O_7 content. A plot of the intensity of the Raman bands versus increasing amount of rhenium per unit surface area for the $\text{Re}_2\text{O}_7/\text{TiO}_2$ and $\text{Re}_2\text{O}_7/\text{Al}_2\text{O}_3$ catalysts are shown in Fig.4.2. For both the samples, the intensity is seen to increase almost linearly with increasing rhenium content up to a certain limit and then attains a constant value. For the $\text{Re}_2\text{O}_7/\text{TiO}_2$ catalysts the linear relationship is observed up to an attempted coverage of $\sim 5\%$ Re_2O_7 and for $\text{Re}_2\text{O}_7/\text{Al}_2\text{O}_3$ catalysts it is up to $\sim 10\%$ Re_2O_7 . At higher coverages the constant value of intensity of the $\sim 1000\text{ cm}^{-1}$ band for both sets of catalysts is due to the loss of the surface rhenia species. From the curves in Fig.4.2, it is evident that the amount of rhenium lost is a function of the initial rhenium content. Hardcastle *et al.* found that the loss of rhenium is a function of both the initial amount of rhenium present and the calcination temperature [18]. The XPS surface studies is also in agreement with the above

findings.

The surface rhenia species present on titania and alumina supports under dehydrated conditions possess bands at $\sim 1000\text{ cm}^{-1}$ and $\sim 973\text{ cm}^{-1}$ in the $700\text{-}1100\text{ cm}^{-1}$ region as observed in the Raman spectra (Figs 3.6 and 3.7). The bands in the first overtone region of the Re=O vibration for the IR spectra also reveal the presence of bands at $1992\text{-}2003\text{ cm}^{-1}$ and $1954\text{-}1974\text{ cm}^{-1}$ region. The presence of these bands is independent of the rhenia loading and oxide support. Comparing these band positions with those obtained under ambient conditions ($\sim 975\text{ cm}^{-1}$ and $\sim 930\text{ cm}^{-1}$) it is seen that under *in situ* conditions there is a shift of the band positions to higher frequencies. This shift is due to the removal of the adsorbed water and formation of a new rhenia structure having an oxygen bridge with the oxide support. Comparison of the Raman and IR spectra of $\text{Re}_2\text{O}_7/\text{Al}_2\text{O}_3$ and $\text{Re}_2\text{O}_7/\text{TiO}_2$ catalysts suggest that under dehydrated conditions the same type of surface rhenia species is present on both the supports.

The assignment of the Raman bands are done by comparing them with reference Raman spectra. The $\sim 1000\text{ cm}^{-1}$ band which is present for all loadings is assigned to a true Re=O terminal bond [20]. Since this bond is present at all loadings and for all supports, there is the same functionality present on the oxide surface. There is an absence of Raman bands at $\sim 450\text{ cm}^{-1}$ and in the $200\text{-}150\text{ cm}^{-1}$ region (not shown in Fig.), characteristic of Re-O-Re linkages, suggesting that the surface rhenium oxide species are isolated. Comparing the spectra with that of $\alpha\text{-Li}_6\text{ReO}_6$ which has an octahedrally (six) coordinated rhenia species shows that the surface species is not octahedral since a peak at 680 cm^{-1} is not observed. The surface rhenia species is thus either four or five

coordinated, isolated and possesses one or more Re=O functionalities.

The Raman and IR spectra also show that the vibration at 1000 cm^{-1} is both Raman and IR active. This indicates that the symmetry is lower than tetrahedral. The surface species, thus possess either a C_{3v} or a C_{2v} symmetry. The presence of a C_{2v} or C_{3v} symmetry depends on the number of Re=O terminal bonds present.

To determine the number of Re=O terminal bonds present in the active species, the information from IR spectra is used. The IR spectra reveals the presence of bands at $1992\text{--}2003\text{ cm}^{-1}$ (symmetric stretching) and $1954\text{--}1974\text{ cm}^{-1}$ (asymmetric stretching). The presence of two bands indicate that more than one (either two or three) terminal Re=O bonds are present for each surface rhenia species. In order to ascertain whether the surface rhenia species has a C_{3v} (3 terminal Re=O bonds) or a C_{2v} (2 terminal Re=O bonds) symmetry the spectra is compared with those of reference compounds. The band positions for compounds like ReO_3Cl , ReO_3Br and ReO_3F possessing C_{3v} symmetry are 1001 , 997 and 1001 cm^{-1} , respectively, while that for ReF_3O_2 having C_{2v} symmetry is 1026 cm^{-1} . The Raman spectra of the $\text{Re}_2\text{O}_7/\text{TiO}_2$ and $\text{Re}_2\text{O}_7/\text{Al}_2\text{O}_3$ catalysts show vibrations at positions lower than the band positions of ReF_3O_2 , but in the region of the bands for ReO_3Cl , ReO_3Br and ReO_3F . Thus, comparison with the reference compounds suggest that the surface rhenia species is four coordinated with C_{3v} symmetry (3 terminal Re=O bonds) rather than C_{2v} (2 terminal Re=O bonds).

4.5 Temperature Programmed Reduction Studies

Temperature Programmed Reduction is a valuable technique for investigating the

reducibility of rhenium catalysts. This technique involves monitoring the removal of oxygen from the catalyst surface by means of hydrogen while the temperature is increased linearly with time. The ease with which the oxygen is removed from the catalyst, i.e., lower the temperature at which the reduction peak maxima occurs gives an indication about the higher reducibility of the catalyst. Detailed information about reducibility is critical because reduction of the surface rhenia species is important during oxidations reactions, and in some cases the catalytically active rhenium sites are created by the reduction of Re^{+7} oxide present on the freshly prepared catalyst.

From Figs. 3.13 and 3.14 it is observed that the TPR peak maxima for the $\text{Re}_2\text{O}_7/\text{Al}_2\text{O}_3$ and $\text{Re}_2\text{O}_7/\text{TiO}_2$ catalysts are distinct. Fig.4.3 shows the change in the TPR reduction peaks with rhenium oxide loading on the surface for the two sets of catalysts. There are two distinct regions for the $\text{Re}_2\text{O}_7/\text{TiO}_2$ and $\text{Re}_2\text{O}_7/\text{Al}_2\text{O}_3$ catalysts at 217°C and 352°C , respectively. It is also evident from the plot that for both the samples the peak maxima remains more or less constant with increase in the rhenium loading. This distinct difference in temperatures for the rhenia species on different supports suggests that the oxygen bonding is different for the two sets of catalysts. Since the Raman spectra of both $\text{Re}_2\text{O}_7/\text{TiO}_2$ and $\text{Re}_2\text{O}_7/\text{Al}_2\text{O}_3$ catalysts show bands at $\sim 1000\text{ cm}^{-1}$ due to the terminal $\text{Re}=\text{O}$ bond, the terminal $\text{Re}=\text{O}$ bond strength for both sets of samples are therefore similar. Consequently, the difference in bonding energy of the oxygen species lies with the $\text{Re}-\text{O}$ -support bond. The peak maxima for the rhenia-titania samples is much lower than that of the rhenia-alumina catalysts. Hence, reducibility of the titania supported samples is more than that of the alumina supported samples. This is in agreement with the

trend observed by Vuurman *et al.* [20]. The Re-O-support bond is thus stronger for the alumina than the titania support.

4.6 Effect of Additives

The effect of vanadium and sodium additives on the surface rhenia species were studied. The Raman spectra of the undoped V_2O_5/TiO_2 and Re_2O_7/TiO_2 samples under dehydrated conditions show that the V=O and Re=O vibrations are different. The V=O vibration is at 1028 cm^{-1} while that for Re=O is at $\sim 1003\text{ cm}^{-1}$. The rhenia-titania samples doped with vanadia show Raman features similar to the pure rhenia-titania sample (band at 1002 cm^{-1}). No distinct peak at $\sim 1028\text{ cm}^{-1}$ is observed for either sample. The absence of the V=O Raman band is due to its lower intensity with respect to the Re=O band. The 5% Re_2O_7 sample that has a relatively lower amount of rhenium, however, has a slight shoulder at $\sim 1025\text{ cm}^{-1}$ which can be attributed to the presence of the V_2O_5 species. The TPR data for vanadia added Re_2O_7/TiO_2 and Re_2O_7/Al_2O_3 catalysts show that the addition of vanadium results in a shift of the reduction peak to slightly higher values. The single, sharp reduction peak is retained and there are no other peaks to show the possibility of a direct interaction of the vanadia with the surface rhenia species. Thus, results of Raman and TPR studies demonstrate that the vanadia species added to the catalyst does not effect the structure of the surface rhenia species but binds to the support directly. Furthermore, there is no compound formation between the vanadia and the rhenia species since the intensity of the surface rhenia species is maintained. The vanadia can be said to be a noninteracting additive on the rhenia-titania and rhenia-alumina catalysts.

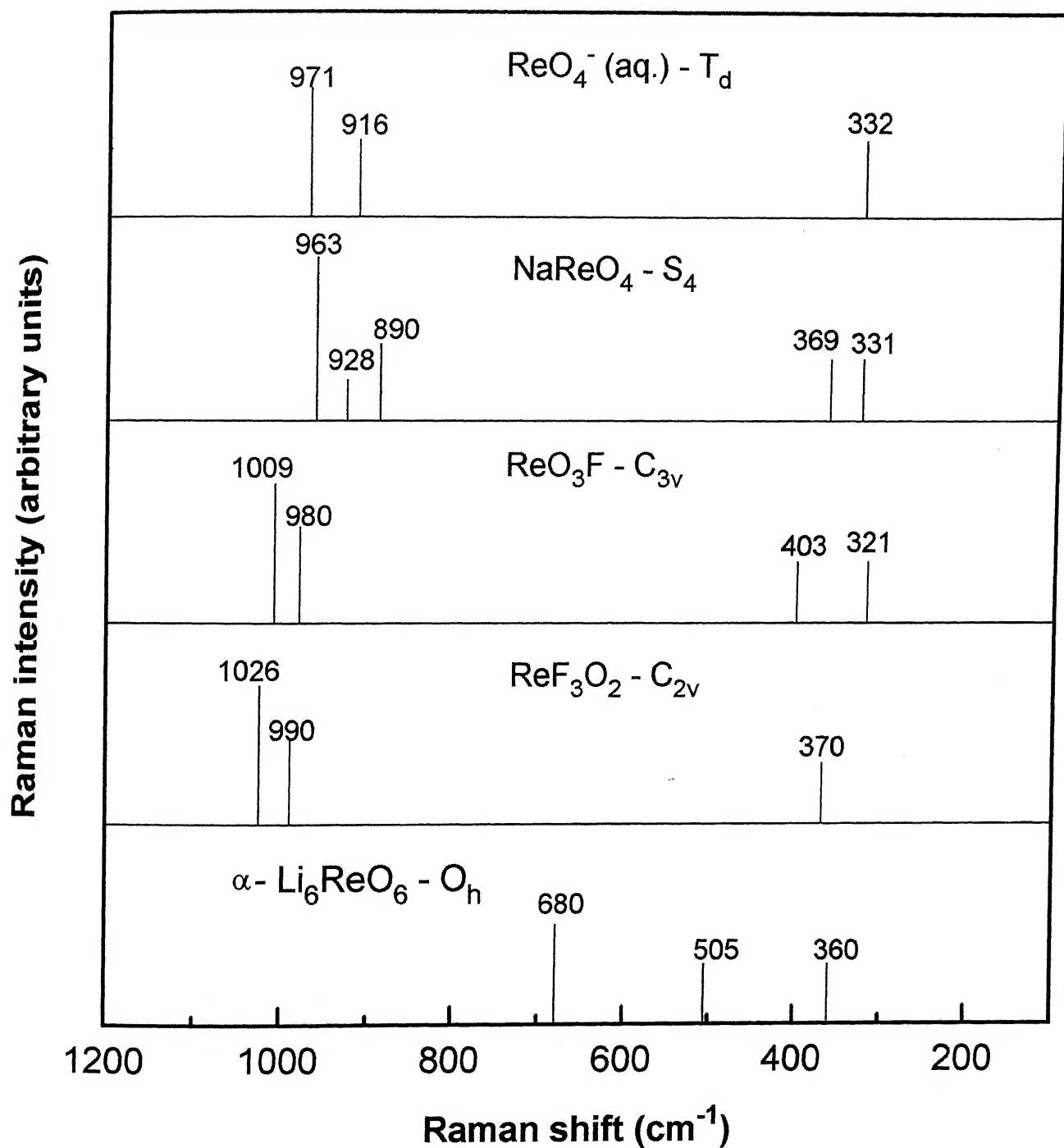


FIG. 4.1 STICK DIAGRAM OF RHENIUM OXIDE REFERENCE COMPOUNDS HAVING DIFFERENT STRUCTURES.

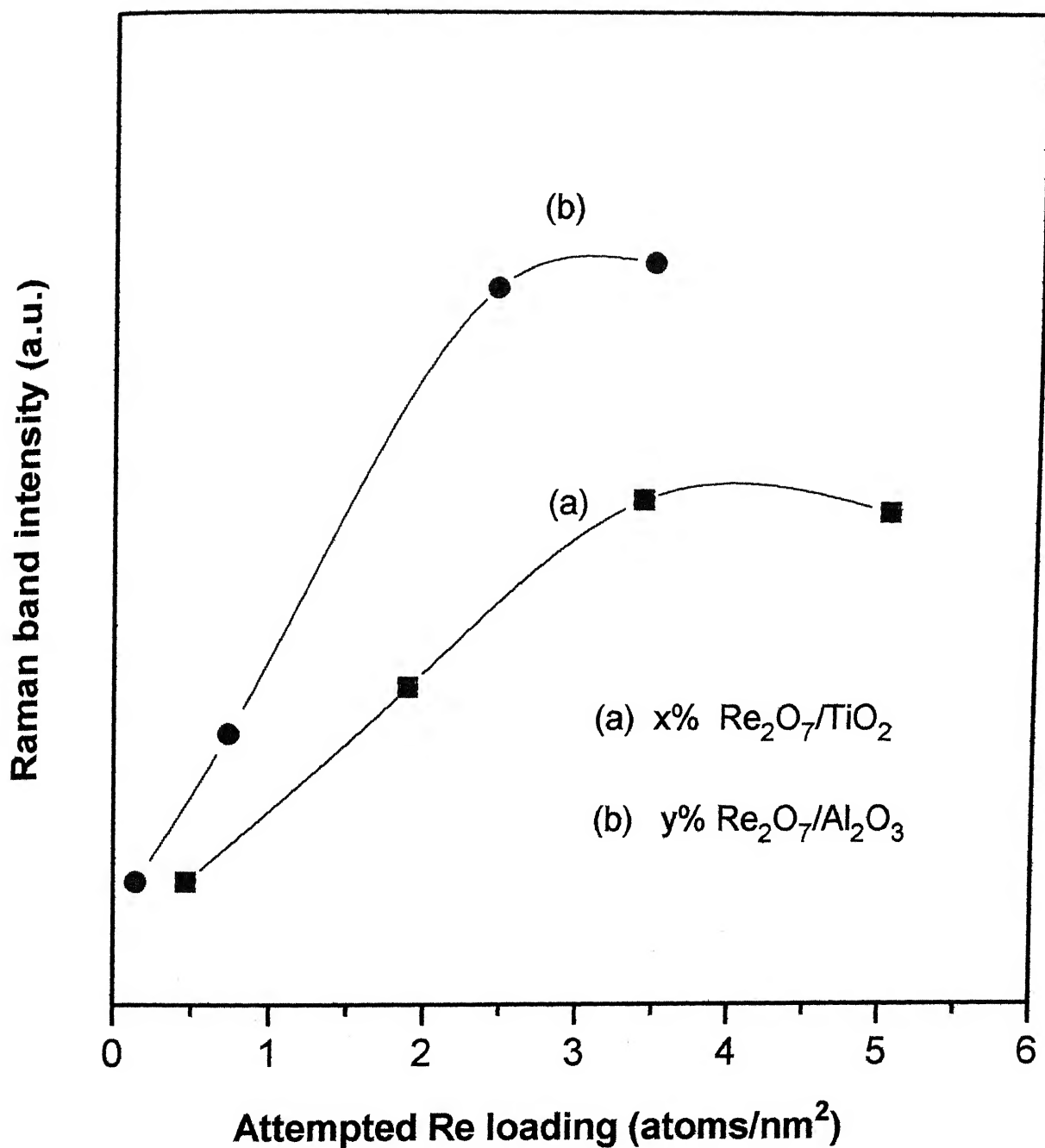


FIG. 4.2 PLOT OF INTENSITY OF THE RAMAN BAND (Re=O STRETCHING VIBRATION) VERSUS ATTEMPTED RHENIA LOADING FOR Re₂O₇/TiO₂ AND Re₂O₇/Al₂O₃ CATALYSTS.

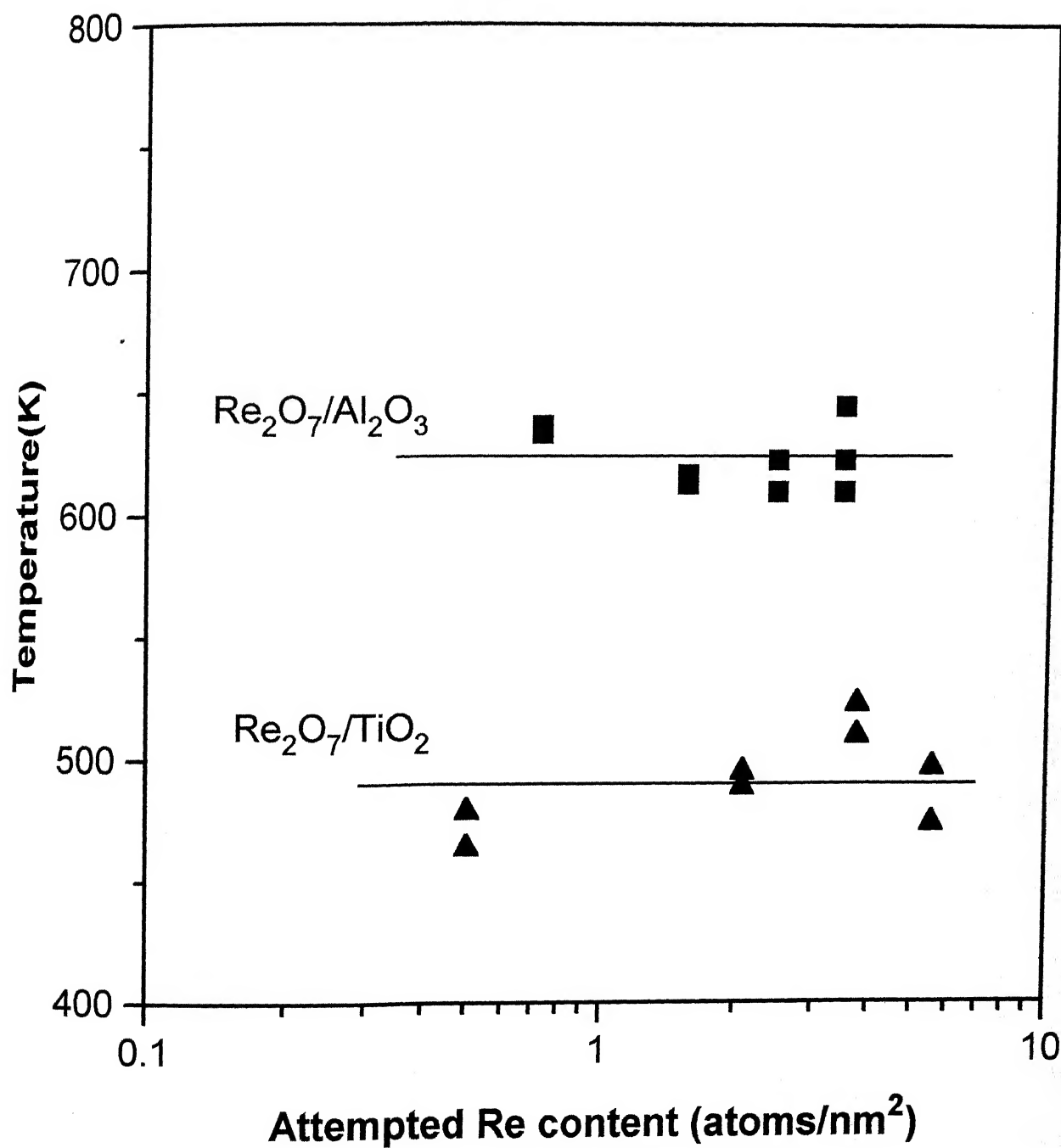


FIG. 4.3 SEMILOG PLOT OF TPR PEAK MAXIMA VERSUS SURFACE CONCENTRATION OF RHENIUM IN THE Re₂O₇/Al₂O₃ AND Re₂O₇/TiO₂ CATALYSTS.

Chapter 5

Conclusions

In this study, the nature of the surface rhenia species on supported rhenia catalysts was determined using various characterization techniques as a function of oxide support, rhenia loading, environment (ambient and dehydrated) and additives. The characterization techniques used were Raman spectroscopy, FTIR spectroscopy, XPS and TPR method and the following conclusions were made.

Supported rhenia catalysts were successfully prepared on TiO_2 and Al_2O_3 supports by the incipient wetness impregnation method using perrhenic acid as the precursor. However, the surface rhenia species could not be formed on the SiO_2 support. This could be due to the presence of fewer reactive surface hydroxyls on the SiO_2 surface and/or the volatility of the surface rhenia species.

XPS studies revealed that the surface rhenia species is well dispersed on the catalyst surface. As a function of rhenia loading, it was observed that the loss of the rhenium from the catalyst surface increases at high rhenia loadings due to the volatility of the rhenia species. It was difficult to speculate about the monolayer limits for the different oxide supports as the actual rhenium content on the surface was not determined.

The structure of the rhenia species on the support surface was determined under ambient and dehydrated conditions using Raman and FTIR spectroscopy. It was observed

that under ambient conditions, the surface rhenium oxide species is isolated, hydrated, independent of surface coverage or support and possesses a structure similar to ReO_4^- species in aqueous solution. Under dehydrated conditions, the structure of the surface rhenia species changes due to the desorption of the surface water. The species under these conditions is four coordinated with a C_{3v} symmetry. Thus, the surface rhenia species possesses three terminal $\text{Re}=\text{O}$ bonds and one bridging $\text{Re}-\text{O}$ -support bond.

Temperature programmed reduction studies revealed that the TPR peak maxima was independent of rhenia loading. Furthermore, the reducibility of the $\text{Re}_2\text{O}_7/\text{TiO}_2$ catalysts was more than the $\text{Re}_2\text{O}_7/\text{Al}_2\text{O}_3$ catalysts as indicated by the low TPR peak maxima for the $\text{Re}_2\text{O}_7/\text{TiO}_2$ catalysts. The reduction proceeded from the +7 valence state to a lower state but not the metal. Since the actual amount of rhenia present was not determined it could not be ascertained whether the final state of the rhenia species was metal or not.

The effect of additives was studied by addition of oxides of vanadium and sodium to the $\text{Re}_2\text{O}_7/\text{TiO}_2$ and $\text{Re}_2\text{O}_7/\text{Al}_2\text{O}_3$ samples. The results of the Raman and TPR studies suggested that there are two types of interactions between the additives and the surface rhenia species. Vanadium acts as a noninteracting additive by directly binding to the oxide support and not significantly affecting the structure of the surface rhenia species. Sodium, however, acts as an interacting additive and poisons the surface rhenium oxide active site by directly coordinating to it.

References

1. J. R. Bartlett, R. P. Cooney, *Spectroscopy of Inorganic-based Materials*, (1987) 187 (R. J. H. Clark, R. E. Hester, Eds.) Wiley, New York.
2. F. D. Hardcastle and I. E. Wachs, *Proc. 9th Intern. Congr. Catal.*, 4 (1988) 1449 (M. S. Phillips and M. Ternan) Chemical Institute of Canada, Ontario.
3. C. L. Thomas, *Catalytic Processes and Proven Catalysis*, Academic Press, New York, (1970).
4. J. C. Mol and J. A. Moulijn, *Advances in Catalysis*, **24** (1975) 131 (D. D. Eley, H. Pines and P. B. Weisz, Eds.) Academic Press, New York.
5. A. A. Olsthoorn and C. Boelhouwer, *J. Catal.*, **44** (1976) 207.
6. J. C. Mol, *J. Mol. Catal.*, **15** (1982) 35.
7. J. Hietala, A. Root and P. Knuuttila, *J. Catal.*, **150** (1994) 46.
8. T. A. Pecoraro and R. R. Chianelli, *J. Catal.*, **67** (1981) 430.
9. R. Thomas, E. M. van Oers, V. H. J. de Beer, J. Medema and J. A. Moulijn, *J. Catal.*, **76** (1982) 241.
10. E. W. Stern, *J. Catal.*, **57** (1979) 390.
11. W. H. Davenport, V. Kollonitsch and C. Kline, *Ind. Eng. Chem.*, **60** (1968) 11.
12. X. Xiaoding, P. Imhoff, G. C. N. van der Aardweg and J. C. Mol, *J. Chem. Soc. Chem. Commun.*, (1985) 273.

13. X. Xiaoding and J. C. Mol, *J. Chem. Soc. Chem. Commun.*, (1985) 631.
14. A. Andreini, X. Xiaoding and J.C. Mol, *Applied Catalysis*, **27** (1986) 31.
15. X. Xiaoding, C. Boelhouwer, J. I. Benecke, D. Vonk and J. C. Mol, *J. Chem. Soc. Farad. Trans. 1*, **82** (1986) 1945.
16. K. P. J. Williams and K. Harrison, *J. Chem. Soc. Farad. Trans.*, **86(9)** (1990) 1603.
17. A. Ellison, G. Diakun and P. Worthington, *J. Mol. Catal.*, **46** (1988) 131.
18. F. D. Hardcastle, I. E. Wachs, J. A. Horsley and G. H. Via, *J. Mol. Catal.*, **46** (1988)
19. L. Wang and W. K. Hall, *J. Catal.*, **82** (1983) 177.
20. M. A. Vuurman, I. E. Wachs, D. J. Stufkens and A. Oskam, *J. Mol. Catal.*, **76** (1992) 263.
21. T. Kawai, K. M. Jiang and T. Ishikawa, *J. Catal.*, **159** (1996) 288.
22. F. P. J. M. Kerkhof, J. A. Moulijn and R. Thomas, *J. Catal.*, **56** (1979) 279.
23. D. S. Kim and I. E. Wachs, *J. Catal.*, **141** (1993) 419.
24. W. N. Delgass, G. L. Haller, R. Kellerman and J. H. Lunsford, *Spectroscopy in Heterogeneous Catalysis*, Academic Press, New York (1979).
25. S. S. Chan, I. E. Wachs, L.L. Murrell, L. Wang and W. K. Hall, *J. Phys. Chem.*, **88** (1984) 5831.
26. A. A. Olsthoorn and C. Boelhouwer, *J. Catal.*, **44** (1976) 197.
27. H. C. Yao and M. Shelef, *J. Catal.*, **44** (1976) 392.
28. Y. V. Maksimov, M. Y. Kushnerev, J. A. Dumesic, A. E. Nechitailo and R. A.

- Fridman, *J. Catal.*, **45** (1976) 114.
29. E. S. Shpiro, V. I. Avaev, G. V. Antoshin, M. A. Ryashentseva and K. M. Minachev, *J. Catal.*, **55** (1978) 402.
30. R. Nakamura, F. Abe and E. Echigoya, *Chem. Lett. Japan Chem. Soc.*, (1981) 51.
31. L. G. Duquette, R. C. Cieslinski, C. W. Jung and P. E. Garrou, *J. Catal.*, **90** (1984) 362.
32. P. Arnoldy, E. M. van Oers, O. S. L. Bruinsma, V. H. J. de Beer and J. A. Moulijn, *J. Catal.*, **93** (1985) 231.
33. P. Arnoldy, O. S. L. Bruinsma and J. A. Moulijn, *J. Mol. Catal.*, **30** (1985) 111.
34. R. M. Edreva-Kardjieva and A. A. Andreev, *J. Catal.*, **94** (1985) 97.
35. R. M. Edreva-Kardjieva and A. A. Andreev, *J. Catal.*, **97** (1986) 321.
36. X. Yide, H. Jiasheng, L. Zhiying and G. Xiexian, *J. Mol. Catal.*, **65** (1991) 275.
37. A. M. Turek, I. E. Wachs and E. DeCanio, *J. Phys. Chem.*, **96** (1992) 5000.
38. R. Spronk, J. A. R. van Veen and J. C. Mol, *J. Catal.*, **144** (1993) 472.
39. G. Deo and I. E. Wachs, *J. Catal.*, **146** (1994) 335.
40. G. Deo and I. E. Wachs, *J. Catal.*, **146** (1994) 323.
41. N. Arora, G. Deo, I. E. Wachs and A. M. Hirt, *J. Catal.*, **159** (1996) 1.
42. J-M. Jehng, G. Deo, B. K. Weckhuysen and I. E. Wachs, *J. Mol. Catal. A: Chemical*, **110** (1996) 41.
43. M. Pal, A. Agarwal, M. B. Patel and H. D. Bist, *J. Raman Spec.*, **15** (1984) 211.
44. L. Burcham and I. E. Wachs, unpublished results.
45. I. R. Beattie and T. R. Gilson, *J. Chem. Soc. (A)*, (1969) 2322.

46. D. S. Kim, I. E. Wachs and K. Segawa, *J. Catal.*, **146** (1994) 268.
47. F. P. J. M. Kerkhof and J. A. Moulijn, *J. Phys. Chem.*, **83** (1979) 1612.
48. M. A. Vuurman, I. E. Wachs and A. M. Hirt, *J. Phys. Chem.*, **95** (1991) 9928.
49. G. Deo and I. E. Wachs, *J. Catal.*, **95** (1991) 5889.
50. M. A. Vuurman, PhD Thesis, Universiteit van Amsterdam, The Netherlands, 1992.
51. C. F. Baes and R. E. Mesmer, *The Hydrolysis of Cations*, Wiley and Sons Inc., New York (1986).

A

125022

Date Slip

This book is to be returned on the
date last stated. 125022

CHE-1997-M-MIT-NAT